

Two-Year Longitudinal Monitoring of Amnesic Mild Cognitive Impairment Patients with Prodromal Alzheimer's Disease Using Topographical Biomarkers Derived from Functional Magnetic Resonance Imaging and Electroencephalographic Activity

Jorge Jovicich^{1*}, Claudio Babiloni^{2,3*}, Clarissa Ferrari⁴, Moira Marizzoni⁵, Davide V. Moretti⁶, Claudio Del Percio⁷, Roberta Lizio², Susanna Lopez², Samantha Galluzzi⁵, Diego Albani⁸, Libera Cavaliere⁵, Ludovico Minati¹, Mira Didic^{9,10}, Ute Fiedler¹¹, Gianluigi Forloni⁸, Tilman Hensch¹², José Luis Molinuevo¹³, David Bartrés Faz^{14,15}, Flavio Nobili^{16,17}, Daniele Orlandi⁵, Lucilla Parnetti¹⁸, Lucia Farotti¹⁸, Cinzia Costa¹⁸, Pierre Payoux¹⁹, Paolo Maria Rossini²⁰, Camillo Marra²⁰, Peter Schönknecht¹², Andrea Soricelli⁷, Giuseppe Noce⁷, Marco Salvatore⁷, Magda Tsolaki²¹, Pieter Jelle Visser²², Jill C Richardson²³, Jens Wiltfang^{11,24,25}, Régis Bordet²⁶, Olivier Blin²⁷, Giovanni B. Frisoni^{5,28} and the PharmaCog Consortium

¹ Center for Mind/Brain Sciences, University of Trento, Italy

² Department of Physiology and Pharmacology "V. Erspamer", Sapienza University of Rome, Rome, Italy

³ Department of Neuroscience, IRCCS-Hospital San Raffaele Pisana of Rome and Cassino, Rome and Cassino, Italy

⁴ Unit of Statistics, IRCCS Istituto Centro San Giovanni di Dio Fatebenefratelli, Brescia, Italy

⁵ Lab Alzheimer's Neuroimaging & Epidemiology, IRCCS Istituto Centro San Giovanni di Dio Fatebenefratelli, Brescia, Italy

⁶ Alzheimer's Epidemiology and Rehabilitation in Alzheimer's disease Operative Unit, IRCCS Istituto Centro San Giovanni di Dio Fatebenefratelli, Brescia, Italy

⁷ IRCCS SDN, Napoli, Italy

⁸ Department of Neuroscience, IRCCS - Istituto di Ricerche Farmacologiche Mario Negri, Milano, Italy

- ⁹ Aix-Marseille Université, INSERM, INS UMR_S 1106, 13005, Marseille, France; Service de Neurologie et Neuropsychologie, APHM Hôpital Timone Adultes, Marseille, France
- ¹⁰ APHM, Timone, Service de Neurologie et Neuropsychologie, APHM Hôpital Timone Adultes, Marseille, France
- ¹¹ LVR-Hospital Essen, Department of Psychiatry and Psychotherapy, Faculty of Medicine, University of Duisburg-Essen, Essen, Germany
- ¹² Department of Psychiatry and Psychotherapy, University of Leipzig, Leipzig, Germany
- ¹³ Alzheimer's disease and other cognitive disorders unit, Neurology Service, ICN Hospital Clinic i Universitari and Pasqual Maragall Foundation Barcelona, Spain
- ¹⁴ Medical Psychology Unit, Department of Medicine, Faculty of Medicine and Health Sciences, University of Barcelona, Barcelona, Spain
- ¹⁵ Institut d'Investigacions Biomèdiques August Pi i Sunyer (IDIBAPS), Barcelona, Spain
- ¹⁶ Neurology Clinic, Department of Neuroscience (DINOEMI), University of Genoa, Italy
- ¹⁷ U.O. Clinica Neurologica, IRCCS Ospedale Policlinico San Martino, Genova, Italy
- ¹⁸ Clinica Neurologica, Università di Perugia, Ospedale Santa Maria della Misericordia, Perugia, Italy
- ¹⁹ ToNIC, Toulouse NeuroImaging Center, Université de Toulouse, Inserm, UPS, France
- ²⁰ Department of Gerontology, Neurosciences & Orthopedics, Catholic University, Policlinic A. Gemelli Foundation-IRCCS, Rome, Italy
- ²¹ 1st University Department of Neurology, AHEPA Hospital, Medical School, Aristotle University of Thessaloniki, Thessaloniki, Makedonia, Greece

²² Department of Neurology, Alzheimer Centre, VU Medical Centre, Amsterdam, The Netherlands

²³ Neurosciences Therapeutic Area, GlaxoSmithKline R&D, Gunnels Wood Road, Stevenage,
United Kingdom

²⁴ LVR-Hospital Essen, Department of Psychiatry and Psychotherapy, Faculty of Medicine,
University of Duisburg-Essen, Essen, Germany

²⁵ Department of Psychiatry and Psychotherapy, University Medical Center (UMG), Georg-August-
University, Goettingen, Germany

²⁶ University of Lille, Inserm, CHU Lille, U1171 - Degenerative and vascular cognitive disorders,
Lille, France

²⁷ Aix Marseille University, UMR-CNRS 7289, Service de Pharmacologie Clinique, AP-HM,
Marseille, France

²⁸ Memory Clinic and LANVIE - Laboratory of Neuroimaging of Aging, University Hospitals and
University of Geneva, Geneva, Switzerland

*These authors contributed equally to this work.

Accepted 17 July 2018

Correspondence to:

Dr. Jorge Jovicich, Center for Mind/Brain Sciences, University of Trento, Trento, Italy. Tel.: +39-0461-28 3064; Fax: +39-0461-28-3066; E-mail: jorge.jovicich@unitn.it

Dr. Claudio Babiloni, Department of Physiology and Pharmacology “Erspamer”, University of Rome “La Sapienza”, Rome, Italy. Tel.: +39-0649910989; Fax: +39-0649910917; E-mail: claudio.babiloni@uniroma1.it

Abstract

Auditory “oddball” event-related potentials (aoERPs), resting state functional magnetic resonance imaging (rsfMRI) connectivity, and electroencephalographic (rsEEG) rhythms were tested as longitudinal functional biomarkers of prodromal Alzheimer’s disease (AD). Data were collected at baseline and four follow-ups at 6, 12, 18, and 24 months in amnesic mild cognitive impairment (aMCI) patients classified in two groups: “positive” (i.e., “prodromal AD”; n=81) or “negative” (n=63) based on a diagnostic marker of AD derived from cerebrospinal samples ($A\beta_{42}/P\text{-tau}$ ratio). A linear mixed model design was used to test functional biomarkers for Group, Time, and Group x Time effects adjusted by nuisance covariates (only data until conversion to dementia was used). Functional biomarkers that showed significant Group effects (“positive” versus “negative”, $p < 0.05$) regardless of Time were 1) reduced rsfMRI connectivity in both the default mode network (DMN) and the posterior cingulate cortex (PCC), both also giving significant Time effects (connectivity decay regardless of Group); 2) increased rsEEG source activity at delta (< 4 Hz) and theta (4-8 Hz) rhythms and decreased source activity at low-frequency alpha (8-10.5 Hz) rhythms; and 3) reduced parietal and posterior cingulate source activities of aoERPs. Time x Group effects showed differential functional biomarker progression between groups: 1) increased rsfMRI connectivity in the left parietal cortex of the DMN nodes, consistent with compensatory effects and 2) increased limbic source activity at theta rhythms. These findings represent the first longitudinal characterization of functional biomarkers of prodromal AD relative to “negative” aMCI patients based on 5 serial recording sessions over 2 years.

Keywords: alpha rhythms, amnesic mild cognitive impairment, biomarkers, clinical trial, electroencephalography, functional magnetic resonance imaging, oddball event-related potentials, PharmaCog project, prodromal Alzheimer’s disease, resting state

INTRODUCTION

The International Working Group has recently made a useful distinction between diagnostic and topographical biomarkers of Alzheimer's disease (AD) for research applications in patients with amnesic mild cognitive impairment (aMCI) due to the prodromal manifestation of the pathology [1]. Diagnostic biomarkers were defined as those measuring *in vivo* intrinsic pathophysiological variables characterizing neurobiologically AD, namely amyloid deposition and neurofibrillary tangles in the brain. They are expected to be present at all stages of the disease, are observable even in the preclinical asymptomatic state, are not necessarily correlated with disease severity, and are indicated for inclusion of AD patients in clinical trial protocols. Diagnostic biomarkers include low doses of $A\beta_{1-42}$ and high doses of total tau (T-tau) or phospho tau (P-tau) in cerebrospinal fluid (CSF) or evidence of significant amyloid deposition and tau aggregation in the brain in maps of positron emission tomography (PET) [2].

In contrast, topographic or progression biomarkers may not be specific of AD neuropathology or absent in early disease stages, but they can be very useful to monitor the progression of the disease in the brain and may be related to the kind and severity of cognitive deficits [1]. Progression markers include hippocampal atrophy or cortical thickness, assessed by structural MRI, and cortical hypometabolism in posterior cingulate, parietal, temporal, and hippocampal regions, measured by FDG-PET [1]. Of note, these topographic biomarkers are limited in the sense that they do not directly measure brain amyloid deposition and neurofibrillary tangles in AD patients, so they cannot be used as primary neuropathological endpoints in the evaluation of AD-modifying agents.

Promising candidates as topographic markers of AD are those reflecting functional aspects of brain neurotransmission, neural synchronization, and connectivity, as human cognition is the result of collective and coordinated processes within brain networks such as segregation and integration of cellular signaling [3–5]. In this line, functional MRIs accompanying a resting state condition in quiet wakefulness (rsfMRI) can be used for the computation of temporal correlations of blood oxygenation level dependent (BOLD) signals between voxels belonging to brain regions as a biomarker of intrinsic (not related to events) functional connectivity between those regions [6,7]. Among various cerebral neural networks emerging from such rsfMRI analysis, the default mode network (DMN) is of interest for clinical applications to AD research, being non-invasive and repeatable over time even in patients with several cognitive deficits. Previous rsfMRI studies have shown that this network includes nodes in posterior and anterior cingulate areas, angular gyri, occipital, and parietotemporal regions [8]. In the resting state condition, the intrinsic DMN functional connectivity may be associated with specific self-related and internal processes that can

be parcellated into several sub-classes including self-awareness or “mental self” [9,10] (defined as the conscious ability of reflecting/monitoring about one’s sense of self regarding one’s abilities, traits, and attitudes that guides behaviors, choices, and social interactions), self-reflective thought [11,12], stimulus-independent thoughts [13], mind-wandering [14], introspection [15], integration of cognitive processes [16], and considering the thoughts and perspectives of others [17–19].

Other candidate topographic biomarkers of AD derive from electroencephalographic (EEG) techniques, which are noninvasive, cost-effective, and can be repeated several times along disease progression without learning effects affecting paradigms using tasks. When compared to fMRI and FDG-PET, EEG techniques recording scalp potentials have a modest spatial resolution of some centimeters but a very high temporal resolution (milliseconds); that temporal resolution is ideal to investigate cortical EEG rhythms at different frequency bands within about 1-40 Hz during a resting state condition (i.e., resting state EEG, rsEEG) and quick brain dynamics reflected by positive and negative voltage peaks within tens to hundreds of milliseconds in response to cognitive-motor events challenging attention, short episodic memory, and sensorimotor integration (i.e., event-related potentials, ERPs). A popular ERP paradigm used to investigate temporal dynamics of neural synchronization underpinning cognitive processes is the auditory oddball task [20]. In such a paradigm, subjects are administered a sequence of sensory stimuli of two classes, namely those with high (e.g., 80%) and low (e.g., 20%) probability to occur, with the instruction to pay attention and react (e.g., hand motor responses or mental stimulus) only to the rare ones considered as “targets” [21]. The extraction of variables of interest from rsEEG and ERPs requires different procedures of data analysis and source estimation, mainly based on frequency (rsEEG) and time (ERP) domains [22]. Derived rsEEG/ERP biomarkers may reflect synchronization and connectivity between large populations of cortical pyramidal neurons during resting state or cognitive tasks [22].

Previous studies have shown that compared to control seniors, patients with aMCI and dementia due to AD were characterized by increased rsEEG power density at delta (< 4 Hz) and theta (4-7 Hz) frequency bands in widespread cortical regions as well as decreased rsEEG power density at alpha (8-13 Hz) and beta (14-30 Hz) frequency bands in central and posterior cortical regions [22–32]. Concerning the oddball paradigm, these patients were characterized by ERP peak latency increase, amplitude decrease, and abnormal topography in a late ample positive component (i.e., P3b). Specifically, P3b peaks at about 300-400 ms from the onset of rare (20-30% of probability) auditory or visual stimuli [33–38]. As topographic biomarkers of progression, these rsEEG/ERP readouts pointed to increased abnormalities in delta/alpha rhythms and P3b peak in aMCI and AD patients with dementia at about 1-year follow up [27,28,34,36]. These effects were

typically discussed in relationship to death of cortical neurons, axonal pathology, and cholinergic neurotransmission deficits [29,39–45].

Linear Mixed Models (R-package lme4) were used as statistical tests as they allow the use of individual longitudinal data sets even when some recording sessions are missing in the series (e.g., for technical failures or patients' problems). The mentioned findings motivate the evaluation of rsfMRI and rsEEG/P3b as topographic biomarkers sensitive to prodromal (MCI) and dementia stages of AD. This process needs to overcome the following methodological limitations of typical multi-centric longitudinal studies: 1) retrospective nature, 2) the use of few recording sessions over time (mostly a baseline and a 1-year follow up) subjected to the confounding effect of disease onset and trajectories in aMCI patients, 3) the lack of a careful characterization of aMCI due to AD as cognitive profile (only one test of episodic memory) and positivity to standard diagnostic biomarkers of AD, and 4) the absence of a control group of aMCI patients not due to AD with expected different disease evolution over time. The European, prospective, multi-centric study entitled "PharmaCog - E-ADNI" (<http://www.pharmacog.org>) addressed such limitations. In the PharmaCog study, 147 aMCI patients were screened as APOE genotyping and AD diagnostic markers of CSF and followed longitudinally with clinical, neuropsychological, MRI, rsEEG/ERP, and blood markers for 24 months. The aMCI patients were separated into two sub-groups, namely those "positive" (i.e., prodromal AD) and "negative" to CSF diagnostic markers of AD (i.e., statistical thresholds for $A\beta_{42}/P\text{-tau}$ ratio based on APOE $\epsilon 4$ carrier status [49]). Preparatory PharmaCog studies described the successful multisite MRI harmonization efforts [46–51] and the characterization of the "positive" and "negative" aMCI subjects as neuropsychological, MRI (i.e., hippocampal atrophy, morphometry, and diffusion), and rsEEG/ERP at the baseline stage [23,52,53].

This article is part of a Mini Forum on PharmaCog matrix of biomarkers of prodromal AD in patients with aMCI, which is based on four papers published in the *Journal of Alzheimer's Disease*. The specific aim of this article is to evaluate longitudinal functional topographical biomarkers derived from rsfMRI and rsEEG/ERP data in a population of aMCI enrolled in the PharmaCog project and test if these markers can differentiate the group of the "positive" aMCI patients with prodromal AD from the "negative" aMCI subgroup during a time window of 24 months with 5 serial recordings 6 months apart. A linear mixed model adjusted by nuisance covariates was used to investigate those functional biomarkers in terms of Group ("positive" versus "negative" differences regardless of time), Time (temporal effects regardless of Group effects), and Time x Group fixed effects (differential progression between the two subgroups). In the experimental design, the observation time (i.e., 24 months) was expected to account for possible

different disease stages in the “positive” and “negative” aMCI patients, while the “negative” aMCI patients were used as a control subgroup. This allowed dissociating, at least in part, cognitive impairment and functional biomarker differences between prodromal and non-prodromal AD in the aMCI subgroups. For sample homogeneity, the statistical design included aMCI data only until conversion to dementia.

MATERIALS AND METHODS

Participants, clinical exams, and neuropsychological tests

Participants’ demographics, clinical, and neuropsychological data have been described in recent PharmaCog studies [23,52,53]. Briefly, 147 aMCI patients were enrolled in 13 European memory clinics of the Innovative Medicine Initiative (IMI) PharmaCog project (<http://www.pharmacog.org>). Follow-up examinations were performed every 6 months for at least 2 years or until patient progressed to clinical dementia. The main inclusion/exclusion criteria were 1) age between 55 and 90 years; 2) complaints of memory loss by the patient, confirmed by a family relative; 3) Mini-Mental State Examination (MMSE) score of 24 and higher; 4) overall Clinical Dementia Rating score of 0.5; 5) score on the logical memory test lower than 1 standard deviation from the age-adjusted mean; 6) 15-item Geriatric Depression Scale score of 5 or lower; and 7) absence of significant other neurologic, systemic or psychiatric illness.

Functional MRI data

The multi-site 3T rsfMRI acquisition and analysis protocols have been described in recent studies from the PharmaCog project, also demonstrating high test-retest reproducibility across the Consortium with the use of harmonized MRI acquisition protocols [48,49]. Briefly, 13 European clinical sites equipped with 3.0T scanners used a harmonized MRI acquisition protocol that included structural 3D T1 images [48] and resting state echo-planar imaging (EPI) sessions using manufacturer-provided sequences [49]. This resulted in a sample of 882 rsfMRI datasets (147 subjects, 6 sessions per subject).

Standard brain data preprocessing was performed using SPM8 (<http://www.fil.ion.ucl.ac.uk/spm>) running under Matlab R2012a (The MathWorks, Inc., Natick MA, USA) and code developed in-house [49]. The main focus of the analysis of rsfMRI data was the functional connectivity within the nodes of DMN, which is expected to be reduced in the early stages of AD [23,54–57]. In this line, DMN nodes of interest for this study were the following: medial prefrontal cortex (MFC), bilateral precuneus and posterior cingulate cortex (PCC), and inferior left and right parietal cortex (LPC and RPC, respectively). We also included the left

attention frontal-parietal (LFP) network given its potential role in memory cognitive reserve [23,58]. The anatomical characteristics of the DMN and LFP regions and the data analysis procedure are reported in previous methodological study of the Consortium [49]. In brief, Group Independent component analysis (ICA) was performed using 10 spatial components on the concatenated data from each MRI site followed by back-reconstruction [59] to derive the single session DMN and attention LFP network from each subject [49]. DMN regions-of-interest (ROIs) for functional connectivity measurements were obtained by thresholding at $z > 4$ the aggregate DMN site component [49]. For each participant and session, this analysis yielded the average connectivity z-score within the whole DMN, LFP, and also considering separately each one of the separate nodes within the DMN (PCC, LPC, RPC, and MFC) [49]. These z-scores were used as functional connectivity measures and were the rsfMRI dependent variables in the statistical analyses.

The statistical analyses considered also two MRI-related nuisance regressors for each session, the white matter temporal signal-to-noise ratio (tSNR), given its high variability across sites mostly driven by hardware differences [49], and the median head movement.

EEG data

Recordings of rsEEG (eyes-closed and -open; $n = 126$) and auditory “oddball” ERPs ($n = 125$) were performed by commercial digital EEG systems in the Clinical Units of the PharmaCog Consortium (see more details in [52]). A minimum of 19 scalp electrodes was positioned according to the international 10–20 montage system and referenced to linked earlobes or cephalic reference according to the constraints of the local EEG systems. Ground electrode was placed over the scalp, according to the local standard of the Clinical Units. To monitor eye movements and blinking, bipolar vertical and horizontal electrooculograms (EOGs; 0.3-70 Hz bandpass) were simultaneously recorded. Furthermore, a standard electrocardiographic (EKG) channel was also recorded by a monopolar V6 derivation to remove possible EKG artifacts from EEG data. All electrophysiological data were digitized in continuous recording mode (from 128 to 1000 Hz sampling rate according to the constraints of the local EEG systems). To minimize drowsiness and sleep onset, the duration of the rsEEG recordings was established subject-by-subject from at least 3 minutes to a maximum 5 minutes for each condition (i.e., eyes closed, eyes open).

The rsEEG and ERP data were segmented and analyzed offline in consecutive 2-s and 3-s epochs, respectively. Artifactual epochs were identified using a computerized home-made automatic software procedure [60], confirmed by two EEG experts (CDP, RL), and then eliminated. Artefact-free rsEEG epochs recorded during eyes open condition were used to control the expected

reactivity of alpha rhythms as a sign of good quality of rsEEG recordings. Artifact-free rsEEG epochs recorded during eyes open condition were used as an input for the analysis of EEG power density spectrum and cortical source estimation. Concerning ERPs, artifact-free ERP epochs related to frequent and rare stimuli were averaged separately to form individual ERPs for those two classes of auditory stimuli. The latency of the posterior P3b peak following rare stimuli was measured at the Pz electrode and used as a latency reference for further analysis. Based on that latency peak, voltage amplitude was measured at all scalp electrodes in both ERPs related to rare stimuli and those related to frequent stimuli. For ERP source estimation, individual P3b peak potential distribution was computed according to a standard procedure as the subtraction of P3b peak voltage for the rare stimuli minus the potential distribution for the frequent stimuli at the same latency.

Official exact low-resolution brain electromagnetic tomography (eLORETA) freeware [61] was used for the estimation of cortical sources of the rsEEG and P3b peak data in a standard brain atlas [61]. This option made the present results replicable by anyone. However, more realistic brain models may ensure more accurate source localizations (e.g., see [62–64]). eLORETA estimated the following rsEEG/P3b peak markers: 1) activity of global and regional (i.e., frontal, central, parietal, occipital, temporal, and limbic lobes as defined in the eLORETA brain atlas [61]) normalized cortical (eLORETA) sources of rsEEG rhythms for delta (2-4 Hz), theta (4-7 Hz), alpha 1 (8-10.5 Hz), delta/alpha 1, and theta/alpha 1 bands, as indexes of cortical neural synchronization; and (2) activity of cortical sources of posterior parietal (i.e., Brodmann areas 5, 7, 39, and 40) and posterior cingulate (Brodmann areas 31 and 23) regions generating P3b peak voltage, as an index of cortical neural synchronization related to attention and short-term auditory episodic memory.

Patients' classification in prodromal AD and control aMCI patients

As mentioned in the Introduction section, the aMCI patients were classified into two subgroups named “positive” (i.e., prodromal AD) and “negative” aMCI based on the results of a Mixture Linear Model with the p sets at < 0.05 [65]. This Model determined the existence of one or more Gaussian populations of aMCI subjects based on the frequency distributions of CSF $A\beta_{42}$ /P-tau levels in the baseline recordings. According to this Model, the aMCI patients were denoted as “positive” aMCI (i.e., prodromal AD) with CSF $A\beta_{42}$ /P-tau levels lower than 15.2 for APOE $\epsilon 4$ carriers and 8.9 for APOE $\epsilon 4$ non-carriers. The remaining aMCI patients were denoted as “negative” aMCI.

Statistical analysis

Statistical analyses were performed using SPSS software for descriptive statistics and R software (A language and environment for statistical computing, version 3.4.1) for the computation of Mixture and Linear Mixed Models. Characteristics of the aMCI participants at the baseline recordings were assessed by parametric t-tests (or corresponding non-parametric Mann-Whitney) for continuous Gaussian (or non-Gaussian) distributed variables ($p < 0.05$) and by Chi-square tests for categorical data ($p < 0.05$).

Linear Mixed Models (R-package lme4) were used as statistical tests as they allow the use of individual longitudinal data sets even when some recording sessions are missing in the series (e.g., for technical failures or patients' problems). Specifically, these models evaluated whether rsfMRI and rsEEG/ERP functional topographic biomarkers can differentiate a "positive" aMCI (prodromal AD) subgroup relative to a "negative" aMCI subgroup over 24 months. Furthermore, two different types of Linear Mixed Models were used with all available values of the rsfMRI, rsEEG/P3b peak, and clinical variables in the whole aMCI cohort. In the Models, the fixed effect Group included the two subgroups of "positive" and "negative" aMCI patients, while the fixed effect Time included the values of rsfMRI, rsEEG/P3b peak, and ADAScog13 for baseline recordings and follow-ups at 6, 12, 18, and 24 months. The aMCI patients eventually progressing to dementia were no more called for subsequent follow ups in order to have a relatively homogeneous sample of data relative to aMCI condition. Random intercept and random slope across the variables were used as random effects in the Models to account for individual differences in the biomarkers and ADAScog13 values at baseline as well as for individual changes of those variables across all aMCI patients over follow-ups. All Models were adjusted for age, sex, and education. The output of the Linear Mixed Models was presented in terms of standardized β coefficient, corresponding p-value and, for the interaction factor only, effect size (pseudo h^2) calculated as ratio of explained variability of interaction effect on total variability of each model.

The first Linear Mixed Models of rsfMRI and EEG biomarkers were conducted with Time, Group, and Time X Group interaction as fixed effects. The rsfMRI biomarkers were adjusted also for median head motion and white matter tSNR. The main interest was focused on functional biomarkers (i.e., rsfMRI, rsEEG/P3b peak) associated with the Group effects (regardless of Time), Time effects (regardless of Group), and the Time X Group interaction (the differential progression of the positive aMCI subgroup relative to the negative aMCI subgroup). Specifically, the Group effect showed functional biomarkers distinguishing the two subgroups of aMCI patients regardless the Time effect, while the Group X Time interaction unveiled those biomarkers characterizing the disease progression over-time in the "positive" aMCI subgroup (i.e., prodromal AD).

The second Linear Mixed Models of rsfMRI and EEG biomarkers tested if those functional biomarkers (independent variable) and Time effects predicted cognitive decline over time in the aMCI subgroups as revealed by ADAS-cog13 scores (dependent variable).

RESULTS

PharmaCog aMCI patients' features

Diagnostic markers of CSF and APOE genotypes were available in 144 out of 147 aMCI patients of the PharmaCog/E-ADNI cohort, thus the final data analyses were performed in 144 patients. The main demographic and clinical characteristics of these 144 aMCI patients are reported in Table 1. All of them underwent rsfMRI acquisitions, while a slightly smaller group underwent to rsEEG/ERP recordings (n = 126 patients). The main demographic and clinical characteristics of them are reported in Table 2. In both Tables, as mentioned above, the aMCI patients were aggregated in subgroups based on the baseline $A\beta_{42}$, phospho tau (P-tau), and total tau (T-tau) values in the CSF as a function of APOE genotype [65]. The two aMCI subgroups were defined according to a standard diagnostic marker of AD in CSF samples ($A\beta_{42}$ /P-tau ratio; [1]), based on the results of a Linear Mixture Model [49].

Table 3 reports the number of aMCI patients who converted to AD or other non-AD pathologies during the PharmaCog study. The “negative” aMCI patient group did not present conversions to dementia due to AD within 24 months, but presented 2-3% of conversions to dementia due to non-AD pathologies at 12-month follow up and 4-5% at 24-month follow up. In contrast, the “positive” aMCI patients (i.e., prodromal AD) showed 11% of conversion to dementia due to AD at 12-month follow up, 27-29% at 24-month-follow up, and no conversion to dementia due to non-AD pathologies within 24 months. These features are compatible with the use of 1 SD as a threshold of memory deficits in the present inclusion criteria [51]. As expected, a substantial percentage of the “positive” aMCI patients (i.e., prodromal AD) of the present study showed APOE $\epsilon 4$ carriers (63%) in line with previous large studies in AD patients [50].

Please insert Tables 1, 2, and 3 about here

rsfMRI measures of functional cortical connectivity in the PharmaCog aMCI patients

Table 4 reports the results of a Linear Mixed Model showing the variance explained in rsfMRI measures of functional cortical connectivity by the fixed effects of Group (“positive” versus “negative” group differences regardless of time), Time (temporal differences regardless of group), and Time X Group interaction (differential progression across groups) in aMCI patients

(PharmaCog population described in Table 3) over the observation time (24 months, 5 recording session 6 months apart).

Concerning Group and Time, rsfMRI functional connectivity in both the DMN and PCC showed significant effects ($p < 0.05$). Specifically, Time effects in DMN and PCC showed a global reduction of functional cortical connectivity over time regardless of Group (DMN: $p = 0.01$, Std $\beta = -0.1$; PCC: $p = 0.05$, Std $\beta = -0.09$), reflecting the progressing impairment of that functional cortical connectivity in the general relation with the worsening of cognitive performance. Furthermore, both DMN and PCC functional connectivity measures also exhibited a significant Group effect pointing to reduced functional cortical connectivity in the “positive” aMCI subgroup (i.e., prodromal AD) compared with the “negative” aMCI subgroup regardless of Time (DMN: $p = 0.01$, Std $\beta = -0.2$; PCC: $p = 0.001$, Std $\beta = -0.3$), reflecting the greater impairment of that functional cortical connectivity in the former than the latter subgroup. Fig. 1 (upper diagrams) illustrates these Group and Time effects of functional connectivity in PCC. The plot displays the mean modeled connectivity in the two subgroups of aMCI patients over the 5 recording sessions. The profile of DMN changes is very similar (results not shown). As it can be seen in Fig. 1 for PCC, the functional connectivity decay in the time interval of the study is similar in both subgroups, which is consistent with the finding of no significant Time X Group interactions in DMN and PCC.

Interestingly, only functional cortical connectivity in the LPC node showed a significant Time X Group interaction, indicating an increase of connectivity over time in the “positive” (i.e., prodromal AD) relative to the “negative” aMCI subgroup ($p = 0.01$, Std $\beta = 0.2$). Fig. 2 (upper diagram) illustrates the mean values of rsfMRI connectivity in LPC in the “positive” (i.e., prodromal AD) and “negative” aMCI subgroups over the 5 recording sessions.

The attention LFP network showed no Group effect or Group X Time interaction ($p > 0.05$). Indeed, the only significant finding was a Time effect indicating a lower functional cortical connectivity over time in the LFP network in both “positive” and “negative” aMCI subgroups ($p = 0.01$, Std $\beta = -0.1$).

Please insert Table 4 and Figures 1 and 2 about here

RsEEG and ERP measures of cortical neural synchronization in the PharmaCog aMCI patients

Table 5 reports the results of a Linear Mixed Model showing the variance explained in rsEEG and ERP measures of cortical neural synchronization (i.e., functional biomarkers) by the fixed effects of Group (“positive” versus “negative” aMCI subgroups as defined by CSF $A\beta_{42}/P$ -tau ratio), Time, and Time X Group interaction in the PharmaCog aMCI patients over the observation

time (24 months, 5 recording sessions 6 months apart). The main interest was focused on the significant Group and Time X Group interaction effects ($p < 0.05$).

Concerning the significant Group effect, 13 rsEEG biomarkers showed higher cortical source activation in the “positive” (i.e., prodromal AD) over the “negative” aMCI subgroup ($p < 0.05$) for frequency bands and ratios (e.g., delta, theta, delta/alpha1, and theta/alpha1) typically associated with abnormally high values in AD patients. The strongest statistical effects were found on global cortical sources of delta rsEEG rhythms ($p = 0.005$, Std $\beta = 0.3$) and limbic cortical sources of theta rsEEG rhythms ($p = 0.004$, Std $\beta = 0.3$). This effect was independent of Time (i.e., the 5 recording sessions). In the same line, two auditory “oddball” ERP biomarkers also pointed to significant Group effects regardless of Time (e.g., P3b peak as difference between ERPs associated with rare minus frequent stimuli). Compared to the “negative” aMCI subgroup, the “positive” aMCI subgroup (i.e., prodromal AD) pointed to lower cortical source activation of P3b peak in posterior parietal ($p = 0.005$, Std $\beta = -0.3$) and posterior cingulate ($p = 0.004$, Std $\beta = -0.2$) regions. Fig. 1 (lower diagrams) illustrates the mean values of global cortical sources of delta rsEEG rhythms and cortical source activation of P3b peak in posterior parietal regions in the two subgroups of PharmaCog aMCI patients over the 5 recording sessions.

Concerning the Time X Group interaction (differential progression between “positive” and “negative” subgroups of aMCI patients), only limbic sources of theta rsEEG rhythms showed a significant effect ($p = 0.046$, Std $\beta = 0.1$). Results pointed to a differential increase of activation in limbic sources of theta rhythms over time in the “positive” (i.e., prodromal AD) compared to the “negative” aMCI subgroup ($p < 0.05$). Fig. 2 (bottom) depicts the mean (\pm SEM) values of those sources in the two subgroups of aMCI patients over the 5 recording sessions.

Please insert Table 5

Correlation of rsfMRI and EEG markers with ADAS-cog13 score in the PharmaCog aMCI patients

Linear Mixed Models were also used to test the correlation of rsfMRI and rsEEG/ERP functional biomarkers with ADAS-cog13 scores in the whole PharmaCog aMCI group (all CSF A β ₄₂/P-tau “positive” and “negative” aMCI patients) and only “positive” aMCI patients (i.e., prodromal AD). These models were used to test whether those functional biomarkers correlated with a steeper cognitive decline over time (as assessed by ADAS-cog13 scores) in the “positive” (i.e., prodromal AD) than “negative” aMCI subgroup. As expected, regardless the kind of the functional biomarkers, the Time effect explained an increase of ADAS-cog13 scores (i.e., sign of

reduced cognitive performance) in the whole group of the aMCI patients over the observation time ($p < 0.001$).

For rsfMRI biomarkers, the increase of ADAS-cog13 score was significantly correlated with a reduction of functional cortical connectivity measured in DMN ($p < 0.003$, whole aMCI group; $p < 0.002$, CSF $A\beta_{42}$ /P-tau “positive” aMCI subgroup), PCC ($p < 0.004$, whole aMCI group; $p < 0.003$, CSF $A\beta_{42}$ /P-tau “positive” aMCI subgroup), and LFP network ($p < 0.032$, CSF $A\beta_{42}$ /P-tau “positive” aMCI subgroup).

For rsEEG-ERP biomarkers, the increase of ADAS-cog13 score was significantly correlated with an increased activation (i.e., neural synchronization) of occipital sources of theta/alpha 1 rsEEG rhythms in the “positive” aMCI subgroup (i.e., prodromal AD; $p = 0.041$), these rhythms being typically augmented in magnitude in AD patients.

As a control analysis, Linear Mixed Models were used for the study of the correlation between rsEEG/ERP functional biomarkers and ADAScog13 score in all PharmaCog aMCI patients without the random intercept and random slope as random effects (namely, without removing the global whole group trend in the worsening of the ADAScog 13 scores over time). The Linear Mixed Models were adjusted for age, sex, and education. Results showed that many rsEEG (e.g., central delta, limbic delta, global delta, limbic theta, global theta, frontal theta/alpha 1, central theta/alpha 1, temporal theta/alpha 1, limbic theta/alpha 1, and occipital theta/alpha 1) and ERP (e.g., parietal and posterior cingulate cortex) functional biomarkers of cortical neural synchronization in the quiet wakefulness (rsEEG) and oddball cognitive task (ERPs) pointed to a significant correlation with ADAS-cog13 score measured over the 5 recording sessions ($p < 0.001$). This control finding remarks the substantial impact of the use of random intercept and random slope as random effects in the present Linear Mixed Models, thus unveiled the strict relationship of the mentioned rsEEG and ERP readouts of cortical neural synchronization with the group worsening of the ADAScog 13 scores over time in the whole PharmaCog population of aMCI patients.

DISCUSSION

Functional topographic biomarkers are of interest because they may reflect early interactions between neuropathological alterations specific to prodromal AD (e.g., extracellular accumulation of $A\beta_{1-42}$ and intracellular aggregation of P-tau in the brain) and the neurophysiological mechanisms of functional cortical connectivity and neural synchronization as measured by rsfMRI and EEG readouts, respectively. In the present longitudinal PharmaCog study, we evaluated rsfMRI and rsEEG/ERP functional topographic biomarkers to characterize those neurophysiological mechanisms in aMCI patients satisfying the recent diagnostic criteria of prodromal AD based on

CSF biomarkers [1,66], compared with aMCI patients possibly due to other pathologies. These patients were followed during a relatively long observation period of 24 months.

Functional biomarkers Group effects

The Linear Mixed Models showed a fixed effect of Group (“positive” versus “negative” aMCI subgroups) on both rsfMRI and EEG (i.e., rsEEG and auditory “oddball” ERPs) topographic biomarkers regardless of Time effects. From a general neurophysiological point of view, this finding suggests that the prodromal AD group can be differentiated from the non-prodromal aMCI group by intrinsic functional connectivity and cortical neural synchronization differences (i.e., at rest), as well as by synchronization differences during the oddball task.

Concerning rsfMRI topographic biomarkers, functional connectivity within the DMN, especially within the PCC, was significantly lower in the “positive” (i.e., prodromal AD) than in the “negative” aMCI subgroup regardless of Time effects, while no group difference was observed in the attention LFP network. This finding complements and extends to the prodromal AD condition a large body of previous rsfMRI evidence of cross-sectional studies pointing to a selective disruption of functional connectivity in DMN regions as possible early functional consequences of amyloid-neurodegenerative cascade on cortical systems underpinning resting state condition and low vigilance in AD patients relative to cognitively intact controls ([23,67–73]; for review, see [74]). As a novelty, the present finding showed a selective disruption of functional connectivity within DMN regions (no difference at an attention frontoparietal network) using a longitudinal study design with several serial recording sessions and a relatively large sample of aMCI patients suffering from prodromal AD ($n = 81$) compared with control aMCI patients not due to AD. Such a control group made the present finding on prodromal AD independent of patients’ cognitive grade (i.e., all patients suffered from an aMCI condition), while the longitudinal design with variable intercepts as random effects minimized the confound of patients’ disease stage in the comparison of the two aMCI subgroups. The present finding has also the robustness of international multicentric studies using harmonized and qualified MRI scanners [49].

On the whole, the design of the present study overcomes the methodological limitations of typical cross-sectional studies comparing biomarkers in cognitively intact subjects and AD patients. Furthermore, it overcomes the methodological limitations of longitudinal studies just based on one follow up (typically after 1 year). On the other hand, some of the methodological limitations of this study have been previously discussed [49]. In particular, the harmonization of the rsfMRI acquisitions across the 3T Consortium resulted in a common acquisition rate of $TR = 2.7$ s for full brain coverage. Full brain sub-second acquisition protocols [54] are possible with simultaneous

multi-slice selection techniques, which are becoming more widely available as product sequences in clinical scanners and maybe preferable in future studies. The use of higher temporal resolution protocols may improve not only the sensitivity and specificity of rsfMRI connectivity estimates but also enable the exploration of advanced markers of cortical network dynamics [76–78].

The rsfMRI and rsEEG recordings of this study were not recorded simultaneously. However, the results from both modalities refer to a very similar patients' psychophysiological condition as induced by instructions to the patients about the "resting state condition", based on a shared standard operating procedure among the PharmaCog recording units. Indeed, lower/increased level of vigilance, directed attention, and global mental efforts during the resting state condition are clearly related to the brain activity reflected by the present rsfMRI and EEG variables [63,79].

Concerning rsEEG topographic biomarkers, the present Linear Mixed Models showed a fixed effect of Group ("positive" and "negative" aMCI) on several variables of interest. Compared with the "negative" aMCI subgroup, the "positive" (i.e., prodromal AD) aMCI subgroup exhibited lower posterior (parietal, occipital, temporal and limbic) source activity of the low-frequency alpha band (8-10.5 Hz) while widespread delta (< 4 Hz) and theta (4-8 Hz) source activity was higher. These results specify in source space and prodromal AD condition a bulk of previous rsEEG evidence showing that AD patients with dementia are characterized by high power in widespread delta and theta rhythms, as well as low power in posterior alpha and/or beta (13-20 Hz) rhythms [25,31,32,45,80–82]. In temporal areas, delta power is also abnormally high in AD patients with dementia in relation to regional hypometabolism and memory deficits [83]. Furthermore, a short-term cholinergic regimen with acetylcholinesterase inhibitors partially normalizes theta [84], alpha [85], and delta [86] rhythms. In the same line, long-term administration of the drug regimen shows beneficial effects on theta and alpha/theta band ratio, especially over the frontal areas [87,88].

Concerning ERP topographic biomarkers, the Linear Mixed Models showed a fixed effect of Group ("positive" and "negative" aMCI) on P3b peak of an auditory "oddball" paradigm. Compared with the "negative" aMCI subgroup, the "positive" (i.e., prodromal AD) aMCI subgroup pointed to lower parietal and posterior cingulate source activities. These findings extend to spatial source localization previous evidence showing that P3b peak amplitude at scalp posterior electrodes was smaller in AD patients than control seniors, as a possible dynamic neural underpinning of abnormal attention and short-term episodic memory information processes. However, these findings did not replicate in the two aMCI subgroups previous slowing of P3b peak latency in aMCI and AD patients with dementia compared with elderly control subjects, even across various "oddball" task difficulties and stimulus modalities [37,89–91]. Those effects were previously discussed as related

to AD pathology for visual and olfactory modalities [20,92]. In contrast, the present findings would suggest that P3b peak latency may preferably reflect physiological aging [93] and general deterioration of cognitive performance across pathological aging rather than specific processes of prodromal AD.

Functional biomarkers Time x Group effects: differential progression profiles

Here the Linear Mixed Models showed a significant interaction between Time (5 recording sessions 6 months apart) and Group (“positive” and “negative” aMCI) on both rsfMRI and rsEEG biomarkers. This interaction suggests that in an aMCI group, differential progression profiles between prodromal and non-prodromal AD may be captured by intrinsic functional connectivity (e.g., rsfMRI biomarkers) and cortical neural synchronization (e.g., rsEEG biomarkers).

Concerning rsfMRI biomarkers, we found that the sensitivity to disease progression in aMCI patients varies across cortical networks. Specifically, we found that functional connectivity in the whole DMN, PCC, and LFP were sensitive to short-term longitudinal decay both in the “positive” prodromal AD and the “negative” (control) aMCI patients. But these networks showed no significant differences in the progression of the connectivity profiles. Instead, functional connectivity in LPC exhibited significant differential effects, with increased functional connectivity over time faster in the “positive” (i.e., prodromal AD) relative to the “negative” aMCI subgroup. Again, this finding stressed the selective feature of this disruption of functional connectivity within DMN regions as compared to the lack of effects in the attention frontoparietal network.

Our longitudinal rsfMRI findings are in good agreement with previous evidence showing both cortical network impairment (connectivity reduction) and compensation (connectivity increase) effects in the DMN in aMCI subjects relative to control seniors, despite gray matter atrophy [54,94–96]. Here we extend those results by confirming similar effects in prodromal AD relative to control aMCI subgroup. Further, the present findings showed a maximum sensitivity of rsfMRI LPC functional connectivity at 2-year follow up, generally consistent with previous longitudinal rsfMRI studies considering baseline and 2-3 year follow-up evaluations in groups of patients with AD dementia and aMCI [54–56,96], the latter sometimes diagnosed only on clinical basis. Interestingly, the present lateralization in the left LPC of the effects of longitudinal disease progression in prodromal AD extends recent findings of a longitudinal rsfMRI study with two measurements 2 years apart in a small population of aMCI patients [95]. Such previous study exhibited sensitivity of functional connectivity between left precuneus and other DMN nodes in accounting for the greater progression of aMCI patients in the group of converters to dementia (n=14) than that of non-converters (n=17) [95]. Another recent longitudinal rsfMRI study (baseline

and 35 month follow up) in aMCI patients evaluated genotype-by-diagnosis interaction effects [23,97]. Using seed-based rsfMRI analyses on the hippocampus, the Authors detected functional cortical connectivity reductions in APOE ϵ 4 carriers and functional cortical connectivity increases in non-carriers. In the light of those findings, the present results should not be interpreted as an indication that rsfMRI functional biomarkers of prodromal AD are limited to DMN nodes. It is reasonable that functional connectivity within the episodic memory brain networks including prefrontal, entorhinal regions, and hippocampus may represent another sensitive dimension in prodromal AD.

Concerning rsEEG biomarkers, the “positive” (i.e., prodromal AD) aMCI subgroup was characterized by increasing limbic source activity of theta rhythms over time. The effect was evident across the serial recordings and robust effects were evident for the progression of prodromal AD in periods of about 12 months. Taking into account the relatively low spatial resolution of the EEG techniques used in the present study (i.e., they cannot disentangle the various limbic regions of cortical midline and medial temporal lobe), this finding suggests a limbic localization of prodromal AD processes affecting the generation of abnormal rsEEG rhythms during the disease progression in aMCI patients. This topographical suggestion is in line with the well-known localization of initial AD physiopathological processes in entorhinal regions, medial temporal lobe, and midline regions of DMN. Furthermore, it provides a neuroanatomical framework to previous rsEEG evidence showing that AD patients with dementia are characterized by high power in widespread scalp regions of delta and theta rhythms, as well as low power in posterior alpha and/or beta (13-20 Hz) rhythms [27,28,32,98,99].

What do rsfMRI and EEG topographic biomarkers tell us about prodromal AD?

The rsfMRI findings of the present study support the general view that at least for two years, prodromal AD is associated with a partial functional cortical disconnection within DMN nodes in the resting state condition. It can be speculated that this functional disconnection might induce an abnormal elaboration of information about self-body milieu and autobiographical memory, thus affecting the sense of self-awareness and continuity of self across time [6,77] (for theories and controversies about the neural basis of consciousness see [101]). This speculation is based on the well-known concept that midline cortical nodes of DMN such as PCC and MPF contribute to the integration of the general functions related to the sense of self-awareness [102,103]. In this line of reasoning, PCC might represent information concerning individual’s own self-beliefs and first-person perspective in adults [104]. Furthermore, structural maturation of the neural connectivity between PCC and MPF in the adolescence accompanies the development of self-related and social-

cognitive functions [105]. Moreover, previous evidence has shown that posterior parietal regions of DMN might contribute to the formation of self-related cognitive representation as a convergence zone binding cortical neural populations involved in the memorization of intermodal details of episodic events concerning the self [106]. Patients with lesions in those parietal regions manifest difficulties in re-experiencing a past autobiographic event when request by experimenters [107]. This speculation encourages the inclusion of cognitive tests probing the richness of the autobiographic memories and self-awareness in prodromal AD patients over time and the analysis with Linear Mixed Models of the correlation between rsfMRI topographic biomarkers of DMN and the performance to those tests.

The rsEEG findings of the present study enlightened neurophysiological mechanisms characterizing prodromal AD patients compared to control aMCI patients. Based on those findings and prior knowledge on the role of thalamocortical loops in the generation of rsEEG rhythms in humans, it can be speculated that in quiet wakefulness, the abnormal delta and theta source activity in prodromal AD is due to an abnormal interaction between thalamic and cortical pyramidal neural populations, associated with a loss of functional connectivity and a sort of functional isolation of parietal, temporal, and occipital cortical modules [108–110]. It can be also speculated that the alteration of this neurophysiological mechanism is responsible for the reduced parietal and posterior cingulate source activity of auditory “oddball” P3b peak in prodromal AD patients enrolled in the present study. Indeed, P3b peak is mostly an expression of cognitive event-related oscillatory response of thalamocortical circuits oscillating at delta and theta frequencies. In this line, previous studies have shown that delta event-related impulse oscillations in response to visual and auditory “oddball” stimuli were attenuated in amplitude in AD patients with dementia compared with control seniors (see for a review [111]). In AD patients with dementia, an abnormal thalamocortical interaction might be due to a cortical blood hypoperfusion and synaptic dysfunction [83,112–119]. Another cause of such an abnormal thalamocortical interaction might be an impairment of the cortical gray matter especially in the posterior regions [29,39,120–126], as well as a lesion in the brain white matter connecting cerebral cortex [2,23].

Another interesting finding of the present study is the characterization of prodromal AD patients by widespread cortical alpha sources estimated in the resting state condition in the wakefulness. A tentative neurophysiological explanation of that finding can be based on the insightful research in cats and mice performed by the group of Dr. Crunelli at the Cardiff University. Based on their research, it can be speculated that the reduction of cortical alpha sources in prodromal AD patients over aMCI control patients might denote a progressive alteration in the interplay of thalamocortical high-threshold, GABAergic (interneurons), thalamocortical relay-mode, and cortical pyramidal

neurons that constitute the complex network regulating the cortical arousal and vigilance in quiet wakefulness in mammals [107–109]. In physiological conditions, Dr. Crunelli's group demonstrated that in wakefulness, glutamatergic and cholinergic signaling to those neurons enhances the generation of thalamocortical and cortical alpha rhythms and produces cycles of excitation and inhibition in thalamic and cortical neurons that might frame perceptual events in discrete snapshots of approximately 70–100 ms during vigilance [107–109].

What is the added value of the present rsfMRI and EEG readouts with reference to the new diagnostic guidelines for research published by the International Working Group-2 [1] and NIA-AA Working Group [66]? Summarizing, those guidelines stated that AD can be recognized *in vivo* by both abnormal “A” biomarkers of A β and “T” biomarkers of phospho tau in the brain, derived from PET or CSF techniques. Furthermore, the new NIA-AA Working Group [66] proposed that early “AD neuropathologic changes” can be revealed *in vivo* by abnormal “A” biomarkers of A β and normal “T” biomarkers. Finally, both International Working Group-2 [1] and NIA-AA Working Group [66] encouraged the characterization of AD subject's brain integrity by “N” biomarkers of neurodegeneration derived from CSF (e.g., T-tau), FDG-PET (e.g., hypometabolism), and structural MRI (e.g., atrophy) techniques. In the PharmaCog project, we followed those guidelines for the diagnosis of the prodromal AD in aMCI patients. As a novelty, here we propose that the present rsfMRI and rsEEG readouts changing over time (e.g., 24 months) in prodromal AD patients may be used to characterize and monitor the effect of the disease on their brain functions, thus enriching the picture disclosed by the guideline biomarkers. Specifically, these readouts may complement “N” biomarkers in future longitudinal clinical studies, revealing effects of the prodromal AD progression and new anti-AD drugs on brain functional connectivity with high spatial resolution (i.e., probing fine spatial features of the functional brain topography) and neural synchronization processes with high temporal resolution (i.e., probing multiple oscillatory features of that synchronization facilitating or inhibiting neural signal processing), respectively. Relative neurophysiological insights may better explain clinical manifestations of the disease and therapy response beyond diagnostic and prognostic purposes. Of note, the present article appears in an editorial Mini Forum of the *Journal of Alzheimer's Disease* together with other articles derived from the same PharmaCog clinical trial. One of these articles reports results of systematic statistical comparisons among structural and functional MRI, rsEEG/ERP, and blood biomarkers in prodromal AD patients.

Conclusions

In the PharmaCog project, auditory “oddball” ERPs, rsEEG, and rsfMRI functional biomarkers were tested in aMCI patients to characterize prodromal AD. The prodromal AD in patients with aMCI was established based on abnormal CSF levels of amyloid and P-tau measured at baseline. To take into account the confounding effect of different disease stages and cognitive grades, we used 5 serial recording sessions over 2 years, controlling of cognitive grade using a control group of aMCI patients supposed not due to AD. Functional biomarkers were able to detect significant Group effects stable over time in the prodromal AD patients compared with the control aMCI subgroup: 1) reduced rsfMRI functional connectivity in the DMN and in the PCC node; 2) increased rsEEG source activity at delta (< 4 Hz) and theta (4-8 Hz) rhythms and decreased source activity at alpha (8-10.5 Hz) rhythms; and 3) reduced parietal and posterior cingulate source activities of P3b peak of ERPs. Functional biomarkers were also able to show Time X Group effects, giving differential progression profiles over time in the prodromal AD subgroup relative to the control aMCI subgroup: 1) increased rsfMRI functional connectivity in the LPC node of the DMN and 2) increased limbic source activity at theta rhythms. Topographical biomarkers may have different sensitivity at different phases of the disease [1,127]. At the present stage, we do not know the neuropathological correlates explaining why some rsfMRI and EEG biomarkers were found to be sensitive to Group effects and others to Group X Time effects over 24 months. Future studies correlating those biomarkers with PET maps of A β ₁₋₄₂ and P-tau accumulation in the brain may enlighten such an explanation. The effects observed in this study may be related to the progression of the neurodegeneration shown by 1) FDG-PET maps of hypometabolism in parietal and medial temporal cortical areas, 2) atrophy of hippocampus, entorhinal, and temporal neocortex, and 3) biomarkers of tau aggregation in the brain as revealed by CSF samples and PET maps.

The present findings represent the first longitudinal characterization of functional topographic biomarkers of prodromal AD. If cross-validated, these findings may be used for the stratification and monitoring of the effects of disease-modifying drugs in aMCI patients suffering from AD. Indeed, topographic biomarkers of brain function as those derived from rsfMRI and EEG (or the magnetoencephalographic counterpart) may be more likely to respond to an effective disease-modifying intervention relative to structural neuroimaging atrophy markers (e.g., cortical or hippocampus atrophy) or topographic biomarkers of brain hypometabolism (e.g., those measured by FDG-PET), which may only partially recover as they are markedly dependent on neurodegeneration [1].

ACKNOWLEDGMENTS

This study has been carried out in the Work Package 5 of PharmaCog project (2010-2015, Grant no. 115009; <http://www.pharmacog.org>). The PharmaCog project was funded by the Innovative Medicine Initiative of European Seventh Framework Program, which was granted by the European Committee (50%) and the European Federation of Pharmaceutical Industries and Associations (50%).

Dr. Giovanni Frisoni's group was supported for the development of this study and extraction of magnetic resonance image (MRI) biomarkers by an in-kind contribution of AstraZeneca AB, Södertälje, Sweden.

Dr. Claudio Babiloni's group was also supported for the extraction of electroencephalographic (EEG) biomarkers by an in-kind contribution of F. Hoffmann-La Roche, Basel, Switzerland.

The Authors are grateful to all members and collaborators of the PharmaCog project and to all amnesic mild cognitive impairment (aMCI) patients who agreed to participate in this study as well as the healthy elderly volunteers who participated in the preliminary harmonization phase of the study.

Authors' disclosures available online (<https://www.j-alz.com/manuscript-disclosures/18-0158r1>).

REFERENCES

- [1] Dubois B, Feldman HH, Jacova C, Hampel H, Molinuevo JL, Blennow K, DeKosky ST, Gauthier S, Selkoe D, Bateman R, Cappa S, Crutch S, Engelborghs S, Frisoni GB, Fox NC, Galasko D, Habert MO, Jicha GA, Nordberg A, Pasquier F, Rabinovici G, Robert P, Rowe C, Salloway S, Sarazin M, Epelbaum S, de Souza LC, Vellas B, Visser PJ, Schneider L, Stern Y, Scheltens P, Cummings JL (2014) Advancing research diagnostic criteria for Alzheimer's disease: the IWG-2 criteria. *Lancet Neurol* **13**, 614–629.
- [2] Agosta F, Scola E, Canu E, Marcone A, Magnani G, Sarro L, Copetti M, Caso F, Cerami C, Comi G, Cappa SF, Falini A, Filippi M (2012) White matter damage in frontotemporal lobar degeneration spectrum. *Cereb Cortex* **22**, 2705–2714.
- [3] Friston KJ (2009) Modalities, modes, and models in functional neuroimaging. *Science* **326**, 399–403.
- [4] Sporns O (2013) Structure and function of complex brain networks. *Dialogues Clin. Neurosci.* **15**, 247–62.
- [5] Deco G, Tononi G, Boly M, Kringelbach ML (2015) Rethinking segregation and integration: contributions of whole-brain modelling. *Nat. Rev. Neurosci.* **16**, 430–9.
- [6] Biswal B, Yetkin FZ, Haughton VM, Hyde JS (1995) Functional connectivity in the motor cortex of resting human brain using echo-planar MRI. *Magn Reson Med* **34**, 537–541.
- [7] Fox MD, Raichle ME (2007) Spontaneous fluctuations in brain activity observed with functional magnetic resonance imaging. *Nat Rev Neurosci* **8**, 700–711.
- [8] Heine L, Soddu A, Gómez F, Vanhaudenhuyse A, Tshibanda L, Thonnard M, Charland-Verville V, Kirsch M, Laureys S, Demertzi A (2012) Resting state networks and consciousness: alterations of multiple resting state network connectivity in physiological, pharmacological, and pathological consciousness States. *Front. Psychol.* **3**, 295.
- [9] Johnson SC, Baxter LC, Wilder LS, Pipe JG, Heiserman JE, Prigatano GP (2002) Neural correlates of self-reflection. *Brain* **125**, 1808–14.
- [10] Lou HC, Luber B, Crupain M, Keenan JP, Nowak M, Kjaer TW, Sackeim HA, Lisanby SH (2004) Parietal cortex and representation of the mental Self. *Proc. Natl. Acad. Sci.* **101**, 6827–6832.
- [11] Gusnard DA, Akbudak E, Shulman GL, Raichle ME (2001) Medial prefrontal cortex and self-referential mental activity: relation to a default mode of brain function. *Proc. Natl. Acad. Sci. U. S. A.* **98**, 4259–64.
- [12] Sheline YI, Barch DM, Price JL, Rundle MM, Vaishnavi SN, Snyder AZ, Mintun MA, Wang S, Coalson RS, Raichle ME (2009) The default mode network and self-referential processes in depression. *Proc. Natl. Acad. Sci.* **106**, 1942–1947.
- [13] McKiernan KA, D'Angelo BR, Kaufman JN, Binder JR (2006) Interrupting the "stream of consciousness": an fMRI investigation. *Neuroimage* **29**, 1185–91.
- [14] Mason MF, Norton MI, Van Horn JD, Wegner DM, Grafton ST, Macrae CN (2007) Wandering Minds: The Default Network and Stimulus-Independent Thought. *Science (80-.)*. **315**, 393–395.
- [15] Goldberg II, Harel M, Malach R (2006) When the brain loses its self: prefrontal inactivation during sensorimotor processing. *Neuron* **50**, 329–39.

- [16] Greicius MD, Krasnow B, Reiss AL, Menon V (2003) Functional connectivity in the resting brain: A network analysis of the default mode hypothesis. *Proc. Natl. Acad. Sci.* **100**, 253–258.
- [17] Raichle ME, MacLeod AM, Snyder AZ, Powers WJ, Gusnard DA, Shulman GL (2001) A default mode of brain function. *Proc. Natl. Acad. Sci.* **98**, 676–682.
- [18] Raichle ME, Snyder AZ (2007) A default mode of brain function: A brief history of an evolving idea. *Neuroimage* **37**, 1083–1090.
- [19] Buckner RL, Andrews-Hanna JR, Schacter DL (2008) The brain's default network: anatomy, function, and relevance to disease. *Ann. N. Y. Acad. Sci.* **1124**, 1–38.
- [20] Polich J, Pitzer A (1999) P300 and Alzheimer's disease: oddball task difficulty and modality effects. *Electroencephalogr Clin Neurophysiol Suppl* **50**, 281–287.
- [21] Clifford JO, Anand S (1997) Tri-axial recording of event-related potentials during passive cognitive tasks in patients with Alzheimer's disease. *Int. J. Neurosci.* **92**, 29–45.
- [22] Babiloni C, Lizio R, Marzano N, Capotosto P, Soricelli A, Triggiani AI, Cordone S, Gesualdo L, Del Percio C (2016) Brain neural synchronization and functional coupling in Alzheimer's disease as revealed by resting state EEG rhythms. *Int J Psychophysiol* **103**, 88–102.
- [23] Agosta F, Dalla Libera D, Spinelli EG, Finardi A, Canu E, Bergami A, Bocchio Chiavetto L, Baronio M, Comi G, Martino G, Matteoli M, Magnani G, Verderio C, Furlan R (2014) Myeloid microvesicles in cerebrospinal fluid are associated with myelin damage and neuronal loss in mild cognitive impairment and Alzheimer disease. *Ann Neurol* **76**, 813–825.
- [24] Koenig T, Prichep L, Dierks T, Hubl D, Wahlund LO, John ER, Jelic V (2005) Decreased EEG synchronization in Alzheimer's disease and mild cognitive impairment. *Neurobiol Aging* **26**, 165–171.
- [25] Babiloni C, Binetti G, Cassetta E, Dal Forno G, Del Percio C, Ferreri F, Ferri R, Frisoni G, Hirata K, Lanuzza B, Miniussi C, Moretti D V, Nobili F, Rodriguez G, Romani GL, Salinari S, Rossini PM (2006) Sources of cortical rhythms change as a function of cognitive impairment in pathological aging: a multicenter study. *Clin Neurophysiol* **117**, 252–268.
- [26] Babiloni C, Cassetta E, Binetti G, Tombini M, Del Percio C, Ferreri F, Ferri R, Frisoni G, Lanuzza B, Nobili F, Parisi L, Rodriguez G, Frigerio L, Gurzi M, Prestia A, Vernieri F, Eusebi F, Rossini PM (2007) Resting EEG sources correlate with attentional span in mild cognitive impairment and Alzheimer's disease. *Eur J Neurosci* **25**, 3742–3757.
- [27] Babiloni C, Del Percio C, Lizio R, Marzano N, Infarinato F, Soricelli A, Salvatore E, Ferri R, Bonforte C, Tedeschi G, Montella P, Baglieri A, Rodriguez G, Fama F, Nobili F, Vernieri F, Ursini F, Mundi C, Frisoni GB, Rossini PM (2014) Cortical sources of resting state electroencephalographic alpha rhythms deteriorate across time in subjects with amnesic mild cognitive impairment. *Neurobiol Aging* **35**, 130–142.
- [28] Babiloni C, Lizio R, Del Percio C, Marzano N, Soricelli A, Salvatore E, Ferri R, Cosentino FI, Tedeschi G, Montella P, Marino S, De Salvo S, Rodriguez G, Nobili F, Vernieri F, Ursini F, Mundi C, Richardson JC, Frisoni GB, Rossini PM (2013) Cortical sources of resting state EEG rhythms are sensitive to the progression of early stage Alzheimer's disease. *J Alzheimers Dis* **34**, 1015–1035.
- [29] Babiloni C, Vecchio F, Del Percio C, Montagnese S, Schiff S, Lizio R, Chini G, Serviddio G, Marzano N, Soricelli A, Frisoni GB, Rossini PM, Amodio P (2013) Resting state cortical electroencephalographic rhythms in covert hepatic encephalopathy and Alzheimer's disease.

J Alzheimers Dis **34**, 707–725.

- [30] Babiloni C, Vecchio F, Lizio R, Ferri R, Rodriguez G, Marzano N, Frisoni GB, Rossini PM (2011) Resting state cortical rhythms in mild cognitive impairment and Alzheimer's disease: electroencephalographic evidence. *J Alzheimers Dis* **26 Suppl 3**, 201–214.
- [31] Huang C, Wahlund L, Dierks T, Julin P, Winblad B, Jelic V (2000) Discrimination of Alzheimer's disease and mild cognitive impairment by equivalent EEG sources: a cross-sectional and longitudinal study. *Clin Neurophysiol* **111**, 1961–1967.
- [32] Jelic V, Johansson SE, Almkvist O, Shigeta M, Julin P, Nordberg A, Winblad B, Wahlund LO (2000) Quantitative electroencephalography in mild cognitive impairment: longitudinal changes and possible prediction of Alzheimer's disease. *Neurobiol Aging* **21**, 533–540.
- [33] Jervis BW, Belal S, Cassar T, Besleaga M, Bigan C, Michalopoulos K, Zervakis M, Camilleri K, Fabri S (2010) Waveform analysis of non-oscillatory independent components in single-trial auditory event-related activity in healthy subjects and Alzheimer's disease patients. *Curr Alzheimer Res* **7**, 334–347.
- [34] Papaliagkas V, Kimiskidis V, Tsolaki M, Anogianakis G (2008) Usefulness of event-related potentials in the assessment of mild cognitive impairment. *BMC Neurosci* **9**, 107.
- [35] Papaliagkas VT, Anogianakis G, Tsolaki MN, Koliakos G, Kimiskidis VK (2010) Combination of P300 and CSF beta-amyloid(1-42) assays may provide a potential tool in the early diagnosis of Alzheimer's disease. *Curr Alzheimer Res* **7**, 295–299.
- [36] Papaliagkas VT, Kimiskidis VK, Tsolaki MN, Anogianakis G (2011) Cognitive event-related potentials: longitudinal changes in mild cognitive impairment. *Clin Neurophysiol* **122**, 1322–1326.
- [37] Polich J, Corey-Bloom J (2005) Alzheimer's disease and P300: review and evaluation of task and modality. *Curr Alzheimer Res* **2**, 515–525.
- [38] Tsolaki AC, Kosmidou V, Kompatsiaris IY, Papadaniil C, Hadjileontiadis L, Adam A, Tsolaki M (2017) Brain source localization of MMN and P300 ERPs in mild cognitive impairment and Alzheimer's disease: a high-density EEG approach. *Neurobiol Aging* **55**, 190–201.
- [39] Babiloni C, Del Percio C, Boccardi M, Lizio R, Lopez S, Carducci F, Marzano N, Soricelli A, Ferri R, Triggiani AI, Prestia A, Salinari S, Rasser PE, Basar E, Fama F, Nobili F, Yener G, Emek-Savas DD, Gesualdo L, Mundi C, Thompson PM, Rossini PM, Frisoni GB (2015) Occipital sources of resting-state alpha rhythms are related to local gray matter density in subjects with amnesic mild cognitive impairment and Alzheimer's disease. *Neurobiol Aging* **36**, 556–570.
- [40] Babiloni C, Del Percio C, Caroli A, Salvatore E, Nicolai E, Marzano N, Lizio R, Cavedo E, Landau S, Chen K, Jagust W, Reiman E, Tedeschi G, Montella P, De Stefano M, Gesualdo L, Frisoni GB, Soricelli A (2016) Cortical sources of resting state EEG rhythms are related to brain hypometabolism in subjects with Alzheimer's disease: an EEG-PET study. *Neurobiol Aging* **48**, 122–134.
- [41] Babiloni C, Frisoni G, Steriade M, Bresciani L, Binetti G, Del Percio C, Geroldi C, Miniussi C, Nobili F, Rodriguez G, Zappasodi F, Carfagna T, Rossini PM (2006) Frontal white matter volume and delta EEG sources negatively correlate in awake subjects with mild cognitive impairment and Alzheimer's disease. *Clin Neurophysiol* **117**, 1113–1129.
- [42] Babiloni C, Pievani M, Vecchio F, Geroldi C, Eusebi F, Fracassi C, Fletcher E, De Carli C, Boccardi M, Rossini PM, Frisoni GB (2009) White-matter lesions along the cholinergic

tracts are related to cortical sources of EEG rhythms in amnesic mild cognitive impairment. *Hum Brain Mapp* **30**, 1431–1443.

- [43] Czigler B, Csikos D, Hidasi Z, Anna Gaal Z, Csibri E, Kiss E, Salacz P, Molnar M (2008) Quantitative EEG in early Alzheimer's disease patients - power spectrum and complexity features. *Int J Psychophysiol* **68**, 75–80.
- [44] Jelles B, Scheltens P, van der Flier WM, Jonkman EJ, da Silva FH, Stam CJ (2008) Global dynamical analysis of the EEG in Alzheimer's disease: frequency-specific changes of functional interactions. *Clin Neurophysiol* **119**, 837–841.
- [45] Jeong J (2004) EEG dynamics in patients with Alzheimer's disease. *Clin Neurophysiol* **115**, 1490–1505.
- [46] Albi A, Pasternak O, Minati L, Marizzoni M, Bartres-Faz D, Bargallo N, Bosch B, Rossini PM, Marra C, Muller B, Fiedler U, Wiltfang J, Roccatagliata L, Picco A, Nobili FM, Blin O, Sein J, Ranjeva JP, Didic M, Bombois S, Lopes R, Bordet R, Gros-Dagnac H, Payoux P, Zoccatelli G, Alessandrini F, Beltramello A, Ferretti A, Caulo M, Aiello M, Cavaliere C, Soricelli A, Parnetti L, Tarducci R, Floridi P, Tsolaki M, Constantinidis M, Drevelegas A, Frisoni G, Jovicich J (2017) Free water elimination improves test-retest reproducibility of diffusion tensor imaging indices in the brain: A longitudinal multisite study of healthy elderly subjects. *Hum Brain Mapp* **38**, 12–26.
- [47] Jovicich J, Marizzoni M, Bosch B, Bartres-Faz D, Arnold J, Benninghoff J, Wiltfang J, Roccatagliata L, Picco A, Nobili F, Blin O, Bombois S, Lopes R, Bordet R, Chanoine V, Ranjeva JP, Didic M, Gros-Dagnac H, Payoux P, Zoccatelli G, Alessandrini F, Beltramello A, Bargallo N, Ferretti A, Caulo M, Aiello M, Ragucci M, Soricelli A, Salvadori N, Tarducci R, Floridi P, Tsolaki M, Constantinidis M, Drevelegas A, Rossini PM, Marra C, Otto J, Reiss-Zimmermann M, Hoffmann KT, Galluzzi S, Frisoni GB (2014) Multisite longitudinal reliability of tract-based spatial statistics in diffusion tensor imaging of healthy elderly subjects. *Neuroimage* **101**, 390–403.
- [48] Jovicich J, Marizzoni M, Sala-Llonch R, Bosch B, Bartres-Faz D, Arnold J, Benninghoff J, Wiltfang J, Roccatagliata L, Nobili F, Hensch T, Trankner A, Schonknecht P, Leroy M, Lopes R, Bordet R, Chanoine V, Ranjeva JP, Didic M, Gros-Dagnac H, Payoux P, Zoccatelli G, Alessandrini F, Beltramello A, Bargallo N, Blin O, Frisoni GB (2013) Brain morphometry reproducibility in multi-center 3T MRI studies: a comparison of cross-sectional and longitudinal segmentations. *Neuroimage* **83**, 472–484.
- [49] Jovicich J, Minati L, Marizzoni M, Marchitelli R, Sala-Llonch R, Bartres-Faz D, Arnold J, Benninghoff J, Fiedler U, Roccatagliata L, Picco A, Nobili F, Blin O, Bombois S, Lopes R, Bordet R, Sein J, Ranjeva JP, Didic M, Gros-Dagnac H, Payoux P, Zoccatelli G, Alessandrini F, Beltramello A, Bargallo N, Ferretti A, Caulo M, Aiello M, Cavaliere C, Soricelli A, Parnetti L, Tarducci R, Floridi P, Tsolaki M, Constantinidis M, Drevelegas A, Rossini PM, Marra C, Schonknecht P, Hensch T, Hoffmann KT, Kuijer JP, Visser PJ, Barkhof F, Frisoni GB (2016) Longitudinal reproducibility of default-mode network connectivity in healthy elderly participants: A multicentric resting-state fMRI study. *Neuroimage* **124**, 442–454.
- [50] Marchitelli R, Minati L, Marizzoni M, Bosch B, Bartres-Faz D, Muller BW, Wiltfang J, Fiedler U, Roccatagliata L, Picco A, Nobili F, Blin O, Bombois S, Lopes R, Bordet R, Sein J, Ranjeva JP, Didic M, Gros-Dagnac H, Payoux P, Zoccatelli G, Alessandrini F, Beltramello A, Bargallo N, Ferretti A, Caulo M, Aiello M, Cavaliere C, Soricelli A, Parnetti L, Tarducci R, Floridi P, Tsolaki M, Constantinidis M, Drevelegas A, Rossini PM, Marra C, Schonknecht P, Hensch T, Hoffmann KT, Kuijer JP, Visser PJ, Barkhof F, Frisoni GB, Jovicich J (2016)

Test-retest reliability of the default mode network in a multi-centric fMRI study of healthy elderly: Effects of data-driven physiological noise correction techniques. *Hum Brain Mapp* **37**, 2114–2132.

- [51] Marizzoni M, Antelmi L, Bosch B, Bartres-Faz D, Muller BW, Wiltfang J, Fiedler U, Roccatagliata L, Picco A, Nobili F, Blin O, Bombois S, Lopes R, Sein J, Ranjeva JP, Didic M, Gros-Dagnac H, Payoux P, Zoccatelli G, Alessandrini F, Beltramello A, Bargallo N, Ferretti A, Caulo M, Aiello M, Cavaliere C, Soricelli A, Salvadori N, Parnetti L, Tarducci R, Floridi P, Tsolaki M, Constantinidis M, Drevelegas A, Rossini PM, Marra C, Hoffmann KT, Hensch T, Schonknecht P, Kuijser JP, Visser PJ, Barkhof F, Bordet R, Frisoni GB, Jovicich J (2015) Longitudinal reproducibility of automatically segmented hippocampal subfields: A multisite European 3T study on healthy elderly. *Hum Brain Mapp* **36**, 3516–3527.
- [52] Galluzzi S, Marizzoni M, Babiloni C, Albani D, Antelmi L, Bagnoli C, Bartres-Faz D, Cordone S, Didic M, Farotti L, Fiedler U, Forloni G, Girtler N, Hensch T, Jovicich J, Leeuwis A, Marra C, Molinuevo JL, Nobili F, Pariente J, Parnetti L, Payoux P, Del Percio C, Ranjeva JP, Rolandi E, Rossini PM, Schonknecht P, Soricelli A, Tsolaki M, Visser PJ, Wiltfang J, Richardson JC, Bordet R, Blin O, Frisoni GB (2016) Clinical and biomarker profiling of prodromal Alzheimer's disease in workpackage 5 of the Innovative Medicines Initiative PharmaCog project: a "European ADNI study." *J Intern Med* **279**, 576–591.
- [53] Nathan PJ, Lim YY, Abbott R, Galluzzi S, Marizzoni M, Babiloni C, Albani D, Bartres-Faz D, Didic M, Farotti L, Parnetti L, Salvadori N, Muller BW, Forloni G, Girtler N, Hensch T, Jovicich J, Leeuwis A, Marra C, Molinuevo JL, Nobili F, Pariente J, Payoux P, Ranjeva JP, Rolandi E, Rossini PM, Schonknecht P, Soricelli A, Tsolaki M, Visser PJ, Wiltfang J, Richardson JC, Bordet R, Blin O, Frisoni GB (2017) Association between CSF biomarkers, hippocampal volume and cognitive function in patients with amnesic mild cognitive impairment (MCI). *Neurobiol Aging* **53**, 1–10.
- [54] Damoiseaux JS (2012) Resting-state fMRI as a biomarker for Alzheimer's disease? *Alzheimers Res Ther* **4**, 8.
- [55] Damoiseaux JS, Prater KE, Miller BL, Greicius MD (2012) Functional connectivity tracks clinical deterioration in Alzheimer's disease. *Neurobiol Aging* **33**, 828 e19-30.
- [56] Binnewijzend MA, Schoonheim MM, Sanz-Arigita E, Wink AM, van der Flier WM, Tolboom N, Adriaanse SM, Damoiseaux JS, Scheltens P, van Berckel BN, Barkhof F (2012) Resting-state fMRI changes in Alzheimer's disease and mild cognitive impairment. *Neurobiol Aging* **33**, 2018–2028.
- [57] Dennis EL, Thompson PM (2014) Functional brain connectivity using fMRI in aging and Alzheimer's disease. *Neuropsychol Rev* **24**, 49–62.
- [58] Franzmeier N, Gottler J, Grimmer T, Drzezga A, Araque-Caballero MA, Simon-Vermot L, Taylor ANW, Burger K, Catak C, Janowitz D, Muller C, Duering M, Sorg C, Ewers M (2017) Resting-State Connectivity of the Left Frontal Cortex to the Default Mode and Dorsal Attention Network Supports Reserve in Mild Cognitive Impairment. *Front Aging Neurosci* **9**, 264.
- [59] Calhoun VD, Adali T, Pearlson GD, Pekar JJ (2001) A method for making group inferences from functional MRI data using independent component analysis. *Hum Brain Mapp* **14**, 140–151.
- [60] Moretti D V, Babiloni F, Carducci F, Cincotti F, Remondini E, Rossini PM, Salinari S, Babiloni C (2003) Computerized processing of EEG-EOG-EMG artifacts for multi-centric studies in EEG oscillations and event-related potentials. *Int J Psychophysiol* **47**, 199–216.

- [61] Pascual-Marqui (2007) Discrete, 3D distributed, linear imaging methods of electric neuronal activity. Part 1: exact, zero error localization. *Clin Neurophysiol* **112**, 7.
- [62] Clifford JO, Williston JS (1992) Three dimensional vector analysis of the spatial components and voltage magnitudes of the P300 response during different attentional states and stimulus modalities. *Int. J. Psychophysiol.* **12**, 1–10.
- [63] Clifford JO, Williston JS (1993) The effects of attention and context on the spatial and magnitude components of the early responses of the event-related potential elicited by a rare stimulus. *Int. J. Psychophysiol.* **14**, 209–26.
- [64] Kickhefel A, Weiss C, Roland J, Gross P, Schick F, Salomir R (2012) Correction of susceptibility-induced GRE phase shift for accurate PRFS thermometry proximal to cryoablation iceball. *Magn. Reson. Mater. Physics, Biol. Med.* **25**, 23–31.
- [65] Marizzoni M, Ferrari C, Galluzzi S, Jovicich J, Albani D, Babiloni C, Didic M, Forloni G, Molinuevo JL, Nobili FM, Parnetti L, Payoux P, Rossini PM, Schönknecht P, Soricelli A, Tsolaki M, Visser PJ, Wiltfang J, Bordet R, Cavaliere L, Richardson J, Blin O, Frisoni GB (2017) CSF biomarkers and effect of apolipoprotein E genotype, age and sex on cut-off derivation in mild cognitive impairment. *Alzheimer's Dement.* **13**, P1319.
- [66] Jack CR, Bennett DA, Blennow K, Carrillo MC, Dunn B, Haeberlein SB, Holtzman DM, Jagust W, Jessen F, Karlawish J, Liu E, Molinuevo JL, Montine T, Phelps C, Rankin KP, Rowe CC, Scheltens P, Siemers E, Snyder HM, Sperling R, Contributors C, Masliah E, Ryan L, Silverberg N (2018) NIA-AA Research Framework: Toward a biological definition of Alzheimer's disease. *Alzheimers. Dement.* **14**, 535–562.
- [67] Zhang HY, Wang SJ, Liu B, Ma ZL, Yang M, Zhang ZJ, Teng GJ (2010) Resting brain connectivity: changes during the progress of Alzheimer disease. *Radiology* **256**, 598–606.
- [68] Gili T, Cercignani M, Serra L, Perri R, Giove F, Maraviglia B, Caltagirone C, Bozzali M (2011) Regional brain atrophy and functional disconnection across Alzheimer's disease evolution. *J Neurol Neurosurg Psychiatry* **82**, 58–66.
- [69] Lau WK, Leung MK, Lee TM, Law AC (2016) Resting-state abnormalities in amnesic mild cognitive impairment: a meta-analysis. *Transl Psychiatry* **6**, e790.
- [70] Petrella JR, Sheldon FC, Prince SE, Calhoun VD, Doraiswamy PM (2011) Default mode network connectivity in stable vs progressive mild cognitive impairment. *Neurology* **76**, 511–517.
- [71] Song J, Qin W, Liu Y, Duan Y, Liu J, He X, Li K, Zhang X, Jiang T, Yu C (2013) Aberrant functional organization within and between resting-state networks in AD. *PLoS One* **8**, e63727.
- [72] Amieva H, Letenneur L, Dartigues J-F, Rouch-Leroyer I, Sourgen C, D'Alchee-Biree F, Dib M, Barberger-Gateau P, Orgogozo J-M, Fabrigoule C (2004) Annual rate and predictors of conversion to dementia in subjects presenting mild cognitive impairment criteria defined according to a population-based study. *Dement. Geriatr. Cogn. Disord.* **18**, 87–93.
- [73] Geifman N, Brinton RD, Kennedy RE, Schneider LS, Butte AJ (2017) Evidence for benefit of statins to modify cognitive decline and risk in Alzheimer's disease. *Alzheimers. Res. Ther.* **9**, 10.
- [74] Zhou J, Liu S, Ng KK, Wang J (2017) Applications of Resting-State Functional Connectivity to Neurodegenerative Disease. *Neuroimaging Clin N Am* **27**, 663–683.
- [75] Feinberg DA, Moeller S, Smith SM, Auerbach E, Ramanna S, Gunther M, Glasser MF,

- Miller KL, Ugurbil K, Yacoub E (2010) Multiplexed echo planar imaging for sub-second whole brain fMRI and fast diffusion imaging. *PLoS One* **5**, e15710.
- [76] de Pasquale F, Corbetta M, Betti V, Della Penna S (2017) Cortical cores in network dynamics. *Neuroimage*.
- [77] Preibisch C, Castrillon GJ, Buhner M, Riedl V (2015) Evaluation of Multiband EPI Acquisitions for Resting State fMRI. *PLoS One* **10**, e0136961.
- [78] Wig GS (2017) Segregated Systems of Human Brain Networks. *Trends Cogn Sci* **21**, 981–996.
- [79] Schwartz S, Vuilleumier P, Hutton C, Maravita A, Dolan RJ, Driver J (2005) Attentional load and sensory competition in human vision: modulation of fMRI responses by load at fixation during task-irrelevant stimulation in the peripheral visual field. *Cereb. Cortex* **15**, 770–86.
- [80] Dierks T, Ihl R, Frolich L, Maurer K (1993) Dementia of the Alzheimer type: effects on the spontaneous EEG described by dipole sources. *Psychiatry Res* **50**, 151–162.
- [81] Dierks T, Jelic V, Pascual-Marqui RD, Wahlund L, Julin P, Linden DE, Maurer K, Winblad B, Nordberg A (2000) Spatial pattern of cerebral glucose metabolism (PET) correlates with localization of intracerebral EEG-generators in Alzheimer's disease. *Clin Neurophysiol* **111**, 1817–1824.
- [82] Ponomareva N V, Selesneva ND, Jarikov GA (2003) EEG alterations in subjects at high familial risk for Alzheimer's disease. *Neuropsychobiology* **48**, 152–159.
- [83] Valladares-Neto DC, Buchsbaum MS, Evans WJ, Nguyen D, Nguyen P, Siegel B V, Stanley J, Starr A, Guich S, Rice D (1995) EEG delta, positron emission tomography, and memory deficit in Alzheimer's disease. *Neuropsychobiology* **31**, 173–181.
- [84] Brassens S, Adler G (2003) Short-term effects of acetylcholinesterase inhibitor treatment on EEG and memory performance in Alzheimer patients: an open, controlled trial. *Pharmacopsychiatry* **36**, 304–308.
- [85] Onofri M, Thomas A, Iacono D, Luciano AL, Di Iorio A (2003) The effects of a cholinesterase inhibitor are prominent in patients with fluctuating cognition: a part 3 study of the main mechanism of cholinesterase inhibitors in dementia. *Clin Neuropharmacol* **26**, 239–251.
- [86] Reeves RR, Struve FA, Patrick G (2002) The effects of donepezil on quantitative EEG in patients with Alzheimer's disease. *Clin Electroencephalogr* **33**, 93–96.
- [87] Kogan EA, Korczyn AD, Virchovsky RG, Klimovizky Ss, Treves TA, Neufeld MY (2001) EEG changes during long-term treatment with donepezil in Alzheimer's disease patients. *J Neural Transm* **108**, 1167–1173.
- [88] Rodriguez G, Vitali P, De Leo C, De Carli F, Girtler N, Nobili F (2002) Quantitative EEG changes in Alzheimer patients during long-term donepezil therapy. *Neuropsychobiology* **46**, 49–56.
- [89] Golob EJ, Irimajiri R, Starr A (2007) Auditory cortical activity in amnesic mild cognitive impairment: relationship to subtype and conversion to dementia. *Brain* **130**, 740–752.
- [90] Polich J, Comerchero MD (2003) P3a from visual stimuli: typicality, task, and topography. *Brain Topogr* **15**, 141–152.
- [91] Rossini PM, Rossi S, Babiloni C, Polich J (2007) Clinical neurophysiology of aging brain:

from normal aging to neurodegeneration. *Prog Neurobiol* **83**, 375–400.

- [92] Morgan CD, Murphy C (2002) Olfactory event-related potentials in Alzheimer's disease. *J Int Neuropsychol Soc* **8**, 753–763.
- [93] van Dinteren R, Arns M, Jongsma MLA, Kessels RPC (2014) P300 development across the lifespan: a systematic review and meta-analysis. *PLoS One* **9**, e87347.
- [94] Qi Z, Wu X, Wang Z, Zhang N, Dong H, Yao L, Li K (2010) Impairment and compensation coexist in amnesic MCI default mode network. *Neuroimage* **50**, 48–55.
- [95] Serra L, Cercignani M, Mastropasqua C, Torso M, Spano B, Makovac E, Viola V, Giulietti G, Marra C, Caltagirone C, Bozzali M (2016) Longitudinal Changes in Functional Brain Connectivity Predicts Conversion to Alzheimer's Disease. *J Alzheimers Dis* **51**, 377–389.
- [96] Bai F, Liao W, Watson DR, Shi Y, Yuan Y, Cohen AD, Xie C, Wang Y, Yue C, Teng Y, Wu D, Jia J, Zhang Z (2011) Mapping the altered patterns of cerebellar resting-state function in longitudinal amnesic mild cognitive impairment patients. *J Alzheimers Dis* **23**, 87–99.
- [97] Ye Q, Su F, Shu H, Gong L, Xie CM, Zhou H, Zhang ZJ, Bai F (2017) Shared effects of the clusterin gene on the default mode network among individuals at risk for Alzheimer's disease. *CNS Neurosci Ther* **23**, 395–404.
- [98] Coben LA, Danziger W, Storandt M (1985) A longitudinal EEG study of mild senile dementia of Alzheimer type: changes at 1 year and at 2.5 years. *Electroencephalogr Clin Neurophysiol* **61**, 101–112.
- [99] Soininen H, Partanen J, Laulumaa V, Helkala EL, Laakso M, Riekkinen PJ (1989) Longitudinal EEG spectral analysis in early stage of Alzheimer's disease. *Electroencephalogr Clin Neurophysiol* **72**, 290–297.
- [100] Weiler M, Northoff G, Damasceno BP, Balthazar MLF (2016) Self, cortical midline structures and the resting state: Implications for Alzheimer's disease. *Neurosci Biobehav Rev* **68**, 245–255.
- [101] Tegmark M (2000) Importance of quantum decoherence in brain processes. *Phys. Rev. E. Stat. Phys. Plasmas. Fluids. Relat. Interdiscip. Topics* **61**, 4194–206.
- [102] Northoff G, Bermpohl F (2004) Cortical midline structures and the self. *Trends Cogn Sci* **8**, 102–107.
- [103] Northoff G, Heinzel A, de Greck M, Bermpohl F, Dobrowolny H, Panksepp J (2006) Self-referential processing in our brain--a meta-analysis of imaging studies on the self. *Neuroimage* **31**, 440–457.
- [104] Ochsner KN, Beer JS, Robertson ER, Cooper JC, Gabrieli JD, Kihlstrom JF, D'Esposito M (2005) The neural correlates of direct and reflected self-knowledge. *Neuroimage* **28**, 797–814.
- [105] Supekar K, Uddin LQ, Prater K, Amin H, Greicius MD, Menon V (2010) Development of functional and structural connectivity within the default mode network in young children. *Neuroimage* **52**, 290–301.
- [106] Shimamura AP (2011) Episodic retrieval and the cortical binding of relational activity. *Cogn Affect Behav Neurosci* **11**, 277–291.
- [107] Berryhill ME (2012) Insights from neuropsychology: pinpointing the role of the posterior parietal cortex in episodic and working memory. *Front Integr Neurosci* **6**, 31.
- [108] Klimesch W (1999) EEG alpha and theta oscillations reflect cognitive and memory

performance: a review and analysis. *Brain Res Brain Res Rev* **29**, 169–195.

- [109] Pfurtscheller G, Lopes da Silva FH (1999) Event-related EEG/MEG synchronization and desynchronization: basic principles. *Clin Neurophysiol* **110**, 1842–1857.
- [110] Steriade M, Llinas RR (1988) The functional states of the thalamus and the associated neuronal interplay. *Physiol Rev* **68**, 649–742.
- [111] Yener GG, Basar E (2013) Biomarkers in Alzheimer’s disease with a special emphasis on event-related oscillatory responses. *Suppl Clin Neurophysiol* **62**, 237–273.
- [112] Rae-Grant A, Blume W, Lau C, Hachinski VC, Fisman M, Merskey H (1987) The electroencephalogram in Alzheimer-type dementia. A sequential study correlating the electroencephalogram with psychometric and quantitative pathologic data. *Arch Neurol* **44**, 50–54.
- [113] Brenner RP, Ulrich RF, Spiker DG, Sclabassi RJ, Reynolds 3rd CF, Marin RS, Boller F (1986) Computerized EEG spectral analysis in elderly normal, demented and depressed subjects. *Electroencephalogr Clin Neurophysiol* **64**, 483–492.
- [114] Stigsby B, Johannesson G, Ingvar DH (1981) Regional EEG analysis and regional cerebral blood flow in Alzheimer’s and Pick’s diseases. *Electroencephalogr Clin Neurophysiol* **51**, 537–547.
- [115] Kwa VI, Weinstein HC, Posthumus Meyjes EF, van Royen EA, Bour LJ, Verhoeff PN, Ongerboer de Visser BW (1993) Spectral analysis of the EEG and 99m-Tc-HMPAO SPECT-scan in Alzheimer’s disease. *Biol Psychiatry* **33**, 100–107.
- [116] Niedermeyer E (1997) Alpha rhythms as physiological and abnormal phenomena. *Int J Psychophysiol* **26**, 31–49.
- [117] Passero S, Rocchi R, Vatti G, Burgalassi L, Battistini N (1995) Quantitative EEG mapping, regional cerebral blood flow, and neuropsychological function in Alzheimer’s disease. *Dementia* **6**, 148–156.
- [118] Rodriguez G, Copello F, Vitali P, Perego G, Nobili F (1999) EEG spectral profile to stage Alzheimer’s disease. *Clin Neurophysiol* **110**, 1831–1837.
- [119] Steriade M (1994) Sleep oscillations and their blockage by activating systems. *J Psychiatry Neurosci* **19**, 354–358.
- [120] Killiany RJ, Moss MB, Albert MS, Sandor T, Tieman J, Jolesz F (1993) Temporal lobe regions on magnetic resonance imaging identify patients with early Alzheimer’s disease. *Arch Neurol* **50**, 949–954.
- [121] Fernandez A, Arrazola J, Maestu F, Amo C, Gil-Gregorio P, Wienbruch C, Ortiz T (2003) Correlations of hippocampal atrophy and focal low-frequency magnetic activity in Alzheimer disease: volumetric MR imaging-magnetoencephalographic study. *AJNR Am J Neuroradiol* **24**, 481–487.
- [122] Delli Pizzi S, Maruotti V, Taylor JP, Franciotti R, Caulo M, Tartaro A, Thomas A, Onofri M, Bonanni L (2014) Relevance of subcortical visual pathways disruption to visual symptoms in dementia with Lewy bodies. *Cortex* **59**, 12–21.
- [123] Delli Pizzi S, Franciotti R, Taylor JP, Esposito R, Tartaro A, Thomas A, Onofri M, Bonanni L (2015) Structural Connectivity is Differently Altered in Dementia with Lewy Body and Alzheimer’s Disease. *Front Aging Neurosci* **7**, 208.
- [124] Delli Pizzi S, Padulo C, Brancucci A, Bubbico G, Edden RA, Ferretti A, Franciotti R,

Manippa V, Marzoli D, Onofrij M, Sepede G, Tartaro A, Tommasi L, Puglisi-Allegra S, Bonanni L (2016) GABA content within the ventromedial prefrontal cortex is related to trait anxiety. *Soc Cogn Affect Neurosci* **11**, 758–766.

- [125] Graff-Radford J, Madhavan M, Vemuri P, Rabinstein AA, Cha RH, Mielke MM, Kantarci K, Lowe V, Senjem ML, Gunter JL, Knopman DS, Petersen RC, Jack Jr. CR, Roberts RO (2016) Atrial fibrillation, cognitive impairment, and neuroimaging. *Alzheimers Dement* **12**, 391–398.
- [126] Sarro L, Senjem ML, Lundt ES, Przybelski SA, Lesnick TG, Graff-Radford J, Boeve BF, Lowe VJ, Ferman TJ, Knopman DS, Comi G, Filippi M, Petersen RC, Jack Jr. CR, Kantarci K (2016) Amyloid-beta deposition and regional grey matter atrophy rates in dementia with Lewy bodies. *Brain* **139**, 2740–2750.
- [127] Frisoni GB, Fox NC, Jack CR, Scheltens P, Thompson PM (2010) The clinical use of structural MRI in Alzheimer disease. *Nat. Rev. Neurol.* **6**, 67–77.

Table 1. Clinical and socio-demographic features of amnesic mild cognitive impairment (aMCI) patients receiving resting state functional magnetic resonance imaging recordings (rsfMRI) in the present study. Patients were stratified into cerebrospinal (CSF) A β ₄₂/P-tau “positive” and “negative” according to APOE4-specific cut-offs for carriers and non-carriers of APOE4 genotyping. See Methods section for more details.

	“Negative” aMCI (n = 63)	“Positive” aMCI (n = 81)	p ^a
Age, mean (Standard Deviation, SD)	68.3 (8.4)	69.8 (6.3)	0.2
Sex, F/M, No.	36/27	46/35	1
Education, mean (SD)	10.0 (4.3)	11.1 (4.4)	0.1
APOE ϵ4 carriers, No. (%)	3 (5)	63 (78)	<0.001
MMSE score, mean (SD)	27.1 (1.8)	26.2 (1.8)	0.006
ADAS-cog13, mean (SD)^{b,c}	19.1 (5.9)	21.6 (8.1)	0.052
CSF biomarkers, mean (SD, pg/ml)			
Aβ₄₂	949 (244)	495 (132)	<0.001
P-Tau	47 (15)	84 (38)	<0.001
T-tau	301 (149)	614 (394)	<0.001

^aAssessed by ANOVA (for continuous Gaussian distributed variables) or Kruskal-Wallis with Dunn correction (for continuous non-Gaussian distributed variables) and Chi-square tests (for categorical variables).

^bRange 0-85, with 0 as the best score.

^cInformation was missing for 1 patient.

MMSE, Mini-Mental State Evaluation; SD, standard deviation; ADAS-cog13, Alzheimer Disease Assessment Scale-Cognitive Subscale, version 13; A β ₄₂, amyloid- β ; APOE, apolipoprotein E; CSF, cerebrospinal fluid; P-tau, tau phosphorylated at threonine 181; T-tau, total tau; SD, standard deviation.

Table 2. Clinical and socio-demographic features of aMCI patients undergone to resting state electroencephalographic (rsEEG) and event-related potential (ERP) recordings in the present study. These patients, a subgroup of those described in Table 1, were stratified into CSF A β ₄₂/P-tau “positive” and “negative” according to APOE4-specific cut-offs for carriers and non-carriers of APOE4 genotyping. See Methods section for more details.

	“Negative” aMCI (n = 54)	“Positive” aMCI (n = 72)	p ^a
Age, mean (Standard Deviation, SD)	68.5 (8.5)	69.9 (6.0)	0.2
Sex, F/M, No.	30/24	42/30	0.8
Education, mean (SD)	9.9 (4.1)	11.0 (4.5)	0.2
APOE ϵ4 carriers, No. (%)	3.7%	77.8%	<0.001
MMSE, mean (SD)	26.3 (2.2)	25.2 (2.2)	0.01
ADAS-cog13, mean (SD)^b	20.2 (6.8)	23.1 (7.7)	0.04
CSF biomarkers, mean (SD, pg/ml)			
Aβ₄₂	932 (253)	500 (132)	<0.001
P-tau	47 (15)	84 (36)	<0.001
T-tau	297 (151)	600 (316)	<0.001

^aAssessed by ANOVA (for continuous Gaussian distributed variables) or Kruskal-Wallis with Dunn correction (for continuous non-Gaussian distributed variables) and Chi-square tests (for categorical variables).

^bRange 0-85, with 0 as the best score.

ADAS-cog13, Alzheimer Disease Assessment Scale-Cognitive Subscale, version 13; A β ₄₂, amyloid- β ; APOE, Apolipoprotein E; CSF, cerebrospinal fluid; P-tau, tau phosphorylated at threonine 181; T-tau, total tau; SD, standard deviation.

Table 3. Number of patients who converted from aMCI to dementia due to AD and other pathologies. These patients were stratified into CSF A β ₄₂/P-tau “positive” and “negative” according to APOE4-specific cut-offs for carriers and non-carriers of APOE4 genotyping. See Methods section for more details.

aMCI patients with rsfMRI recordings		
	CSF Aβ₄₂/P-tau “negative” aMCI group	CSF Aβ₄₂/P-tau “positive” aMCI group
n	63	81
Converted in AD (12 months)	0.0% (n=0)	11.1% (n=9)
Converted in AD (24 months)	0.0% (n=0)	27.2% (n=22)
Converted in other dementias (12 months)	3.2% (n=2)	0.0% (n=0)
Converted in other dementias (24 months)	4.8% (n=3)	0.0% (n=0)

aMCI patients with rsEEG/ERP recordings		
	CSF Aβ₄₂/P-tau “negative” aMCI group	CSF Aβ₄₂/P-tau “positive” aMCI group
n	54	72
Converted in AD (12 months)	0.0% (n=0)	11.1% (n=8)
Converted in AD (24 months)	0.0% (n=0)	29.2% (n=21)
Converted in other dementias (12 months)	1.9% (n=1)	0.0% (n=0)
Converted in other dementias (24 months)	3.7% (n=2)	0.0% (n=0)

Table 4. Resting state fMRI nodes showing significant functional connectivity effects explained by a Linear Mixed Model of longitudinal changes (baseline, 6, 12, 18, 24 months follow ups) in aMCI patients stratified into two groups (“positive” as prodromal AD and “negative” as a control group). The model included Group ($A\beta_{42}/P$ -tau ratio), Time, and Time X Group interaction as main predictors of interest adjusted by age, sex, baseline MMSE score, temporal signal-to-noise ratio, and mean fractional head displacement as nuisance variables. Significant ($p < 0.05$) fixed effects are emphasized in bold. DMN, default mode network (all nodes); PCC, posterior cingulate cortex; LPC, inferior left parietal cortex; LFP, left attention frontal-parietal network; Std β , standardized β coefficient of Linear Mixed Model.

rsfMRI connectivity measure	Group		Time		Time X Group	
	Std β	p	Std β	p	Std β	p
PCC	-0,296	0,001	-0,089	0,040	-0,053	0,500
LPC	0,167	0,080	-0,063	0,130	0,186	0,013
DMN	-0,228	0,010	-0,101	0,015	0,012	0,877
LFP	-0,002	0,987	-0,131	0,011	0,030	0,747

Table 5. Resting state EEG and auditory oddball ERP measures showing significant cortical neural synchronization effects explained by a Linear Mixed Model of longitudinal changes (baseline, 6, 12, 18, 24 months follow ups) in aMCI patients stratified into two groups (“positive” as prodromal AD and “negative” as a control group). ERP component of interest was the P3b peak as difference between ERPs peaking about 400 ms post-stimulus associated with rare minus frequent stimuli. The model included Group (A β 42/P-tau ratio), Time, and Time X Group interaction as main predictors of interest adjusted by age, sex and baseline MMSE score as nuisance variables. Significant ($p < 0.05$) fixed effects are emphasized in bold. Std β , standardized β coefficient of the Linear Mixed Model.

rsEEG/ERP measures	Group		Time		Time X Group	
	Std β	p	Std β	p	Std β	p
Central delta rsEEG	0.243	0.014	-0.031	0.515	0.124	0.165
Temporal delta rsEEG	0.228	0.044	0.027	0.563	0.054	0.540
Limbic delta rsEEG	0.235	0.031	0.045	0.292	0.056	0.485
Global delta rsEEG	0.296	0.005	0.000	0.991	0.110	0.145
Limbic theta rsEEG	0.263	0.004	-0.017	0.633	0.138	0.046
Global theta rsEEG	0.232	0.020	-0.021	0.602	0.118	0.124
Parietal delta/alpha1 rsEEG	0.212	0.038	-0.056	0.159	0.107	0.156
Frontal theta/alpha1 rsEEG	0.201	0.045	0.003	0.950	0.059	0.513
Central theta/alpha1 rsEEG	0.266	0.009	-0.020	0.639	0.119	0.132
Occipital theta/alpha1 rsEEG	0.188	0.049	-0.067	0.103	0.146	0.060
Temporal theta/alpha1 rsEEG	0.234	0.016	-0.049	0.258	0.138	0.095
Limbic theta/alpha1 rsEEG	0.256	0.010	-0.013	0.756	0.134	0.088
Global theta/alpha1 rsEEG	0.246	0.013	-0.037	0.390	0.134	0.099
Parietal P3b peak	-0.277	0.005	0.030	0.549	-0.162	0.085
Posterior cingulate P3b peak	-0.250	0.017	0.031	0.598	-0.166	0.136

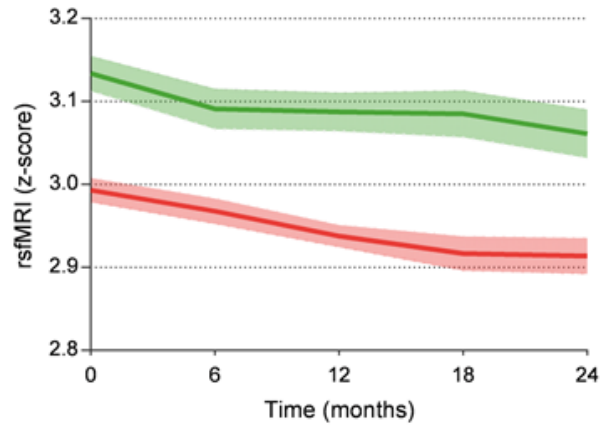
Figure Legends

Fig. 1. Longitudinal profile of functional topographical biomarkers showing significant Group effects regardless of time ($p < 0.05$). Patients were stratified in two amnesic mild cognitive impairment (aMCI) subgroups: $A\beta_{42}/P$ -tau “positive” (red) as prodromal AD as an experimental subgroup and $A\beta_{42}/P$ -tau “negative” (green) as a control subgroup. Mean (\pm standard error of the mean, SEM) model values are shown from 5 recording sessions starting at time zero (baseline) and 6-, 12-, 18-, and 24-month follow-ups. Top: resting state functional magnetic resonance imaging (rsfMRI) functional connectivity measures in the precuneus and posterior cingulate cortex (PCC) of the DMN. Of note, functional rsfMRI connectivity in both PCC and global default mode network (DMN; not shown) gave a similar pattern of significant Group effects (connectivity reduction in “positive” group regardless of time) and Time effects (functional decay in Time regardless of Group, $p < 0.05$). Middle: Mean (\pm standard error of the mean, SEM) values of global cortical sources of resting state electroencephalographic (rsEEG) rhythms at delta frequency band (< 4 Hz). Bottom: mean (\pm SEM) values of parietal cortical sources of auditory “oddball” event-related potentials (ERPs) peaking at about 400 ms (P3b peak) post-stimulus following rare minus frequent stimuli in those groups.

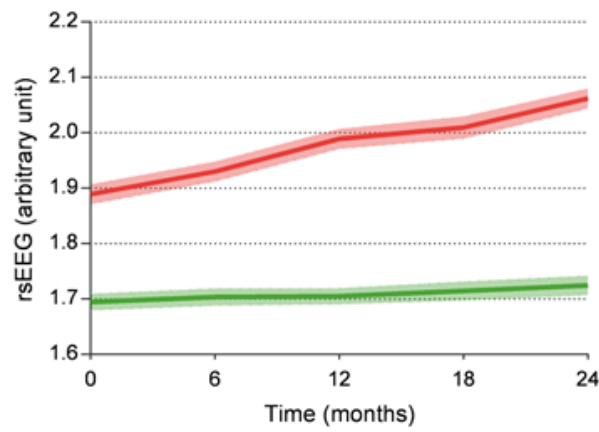
Fig. 2. Longitudinal profile of functional topographical biomarkers showing significant Time \times Group effects ($p < 0.05$). Patients were stratified in two aMCI groups: $A\beta_{42}/P$ -tau “positive” (red) as prodromal AD and $A\beta_{42}/P$ -tau “negative” (green) as a control group. Mean (\pm standard error of the mean, SEM) model values are shown from 5 recording session starting at time zero (baseline) and 6-, 12-, 18-, and 24-month follow-ups. Time \times Group effects show differential progression in the two groups. Top: rsfMRI functional connectivity measures in the left parietal cortex (LPC) of the DMN, showing a progression towards increased connectivity in the “positive” aMCI subgroup relative to the “negative” aMCI subgroup. Bottom. Mean (\pm SEM) values of cortical limbic sources of rsEEG rhythms at theta frequency band (4-8 Hz), showing an increase in cortical neural synchronization in the “positive” (i.e., prodromal AD) subgroup relative to the “negative” aMCI control subgroup.

Fig. 1

Functional rsfMRI connectivity in posterior cingulate cortex



Cortical global delta sources of rsEEG rhythms



Cortical parietal sources of auditory oddball P3b peak

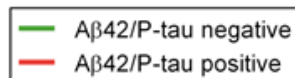
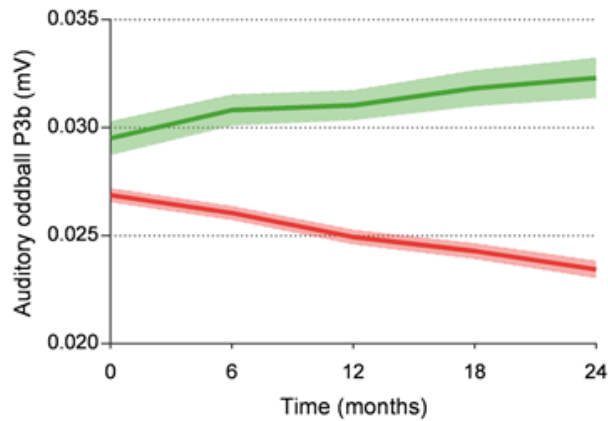
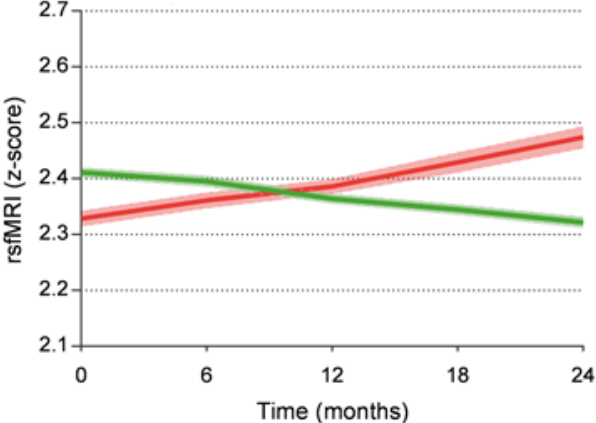


Fig. 2

Functional rsfMRI connectivity in left parietal cortex



Cortical limbic theta sources of rsEEG rhythms

